Dead Leaf Butterfly Optimizer: A novel optimization algorithm for engineering optimization and medical diagnosis based on graph neural network

Dedai Wei
Shenyang University
Min Wan
Nanchang Jiaotong Institute
Xinye Sha
Columbia University
Jiechao Chen
Guang zhou College of Technology and Business
Jiawei Wang
Xiamen Medical College
Wanting Xiao
Zhejiang University School of Medicine
Shengwei Fu
Ministry of Education, Guizhou University
Minyu Qiu
China Jiliang University
Kaichen Ouyang
oykc@mail.ustc.edu.cn

University of Science and Technology of China

Research Article

Keywords: Graph Convolutional Networks, Dead Leaf Butterfly Optimizer, Numerical optimization, Engineering design, Breast Cancer Detection.

Posted Date: March 17th, 2025

DOI: https://doi.org/10.21203/rs.3.rs-6176013/v1

Additional Declarations: No competing interests reported.

Dead Leaf Butterfly Optimizer: A novel optimization algorithm for engineering optimization and medical diagnosis based on graph neural network

Dedai Wei[a, +], Min Wan[b, +], Xinye Sha[c], Jiechao Chen[d], Jiawei Wang[e], Wanting Xiao[f], Shengwei Fu[g],Minyu Qiu[h], Kaichen Ouyang [i, *]

（Dedai Wei and Min Wan contributed equally to this work.）

[a]College of Economics, Shenyang University, Shenyang 110000, China

wdd31212@163.com

[b]Nanchang Jiaotong Institute, Jiangxi Province, Nanchang 330100, China

05050@ncjti.edu.cn

[c]Graduate School of Arts and Sciences, Columbia University, NY 10027, United States of America

xs2399@columbia.edu

[d]College of Management, Guang zhou College of Technology and Business, Foshan 528000, China

jiechaochen629@gmail.com

[e]Department of Clinical Medicine，Xiamen Medical College，Xiamen 361000，China

wjweeii@163.com

[f]Department of Breast and Thyroid Surgery, Affiliated Jinhua Hospital, Zhejiang University School of Medicine, Jinhua 321000, Zhejiang, China

xiaowt7@163.com

[g]Key Laboratory of Advanced Manufacturing Technology, Ministry of Education, Guizhou University, Guiyang, Guizhou 550025, China

shengwei_fu@163.com

[h]Department of Information Engineering, China Jiliang University, Hangzhou 310018, China

minyuqiu@foxmail.com

[i, *]Department of Mathematics, University of Science and Technology of China, Hefei 230026, China

oykc@mail.ustc.edu.cn

*Corresponding author: Kaichen Ouyang (oykc@mail.ustc.edu.cn)

Abstract: Traditional optimization methods often face the problem of local optima, where the optimization process may get trapped in a local optimum, making it difficult to find the global optimal solution. Additionally, these methods tend to have low computational efficiency, especially when dealing with large-scale and complex problems, leading to high time and resource consumption. To address these challenges, we propose an innovative metaheuristic algorithm—Dead Leaf Butterfly Optimizer (DLBO). The algorithm is inspired by the behavior of dead leaf butterflies, mimicking their ability to protect themselves through color changes and camouflage, as well as altering the color of their dorsal surface by spreading their wings to ward off predators. The dead leaf butterfly hides itself from predators by mimicking the shape and color of dead leaves. When it gets threatened or in danger, it spreads its wings to reveal vibrant colors and patterns on its back, creating a visual contrast to deter and surprise enemies. The mix of camouflage and deterrence helps the dead leaf butterfly with great survival abilities. DLBO introduces a new optimization method that effectively avoids getting stuck in local optima and effectively improves global search capabilities. To assess the effectiveness of DLBO, we first compared it with 11 high-performance optimization algorithms on the CEC2017 and CEC2022 benchmark datasets. The results showed that DLBO performed better than other competitors in both convergence and robustness. Next, DLBO was applied to five real-world engineering challenges, including compression spring design, pressure vessel design, multi-disc clutch brake design, and robot gripper optimization. The experimental outcomes showed that DLBO performed excellently in dealing with convoluted engineering problems. Finally, we carried out experiments based on a breast cancer dataset, optimizing the hyperparameters of the Graph Convolutional Networks (GCNs) model with the help of DLBO and 11 other algorithms. GCNs are deep learning models specifically made for graph-structured data analysis, commonly used in biomedical and engineering tasks. Although GCNs can handle complex datasets well, their performance significantly relies on hyperparameter tuning and optimization. The experimental outcomes showcased that DLBO can significantly improve the predictive accuracy of GCNs when applied to breast cancer feature extraction and classification tasks. This study highlights both the strong optimization capabilities of DLBO but also shows the broad usefulness of GCNs in analyzing complex biomedical data.

Keywords: Graph Convolutional Networks; Dead Leaf Butterfly Optimizer; Numerical optimization; Engineering design; Breast Cancer Detection.

1. Introduction

An optimization algorithm is a step-by-step method used to figure out the optimal solution for a specific

optimization task [1, 2]. With the rapid growth of difficulties in real-world challenges, academia and industry confront optimization problems with booming complexity [3, 4]. These problems range from designing efficient algorithms for large-scale data processing to finding cost-effective and sustainable solutions in logistics and supply chain management [5, 6]. Since the introduction of Artificial Intelligence, optimization has been the focus of research as it is particularly difficult to settle real world optimization problems with traditional methods [7-9]. The problem typically involves finding the maximum or minimum value of a function within a defined set of variables, constraints, and priorities, in optimization problems, priority refers to the importance of different objectives or constraints in the decision-making process. The setting of these priorities can affect the final solution. This process requires a deep understanding of the underlying problem structure and the interplay between various factors influencing the objective function [10-12]. Currently, traditional optimization algorithms include Linear Programming [13], Nonlinear Programming, Dynamic Programming [14, 15], Gradient-Based Algorithms [7, 16], etc. These algorithms are widely used in different areas, such as engineering design, economics and finance, operations research, etc. [9, 17, 18]. These traditional algorithms are powerful tools that help in finding the best solutions to complex problems by systematically exploring possible solutions within the constraints of the problem [19, 20]. However, they do have several limitations that can impact their effectiveness when real-world problems are getting more and more complicated [6, 21, 22]. For instance, they often struggle with high-dimensional data or large datasets. High-dimensional problems are characterized by a large number of variables, making the search space exponentially larger and more difficult to solve [5, 16]. Additionally, these conventional approaches, like gradient descent and linear programming, to solving problems in a linear manner are sensitive to initial conditions; a poor initial starting point can lead to slow convergence or even failure to find the optimum [5, 16]. This sensitivity can be particularly problematic in scenarios where the optimization landscape contains numerous local optima [23, 24]. Metaheuristics, a kind of stochastic algorithms, outperform traditional optimization algorithms in real-world optimization problems [11, 25]. These algorithms are high-level procedures designed to find sufficiently good solutions within a reasonable amount of time, making them suitable for large-scale or complex problems (such as combinatorial optimization problems). In these cases, although exact methods can be successfully applied in certain specific situations, they often prove inefficient when dealing with the scale and complexity of the problems. [26, 27]. Metaheuristic algorithms have been applied to various fields, such as bioinformatics, transportation and logistics, manufacturing, etc. In bioinformatics, they help in tasks like sequence alignment, protein structure prediction, and gene expression analysis [5, 6, 15]. In transportation and logistics, they optimize routes, schedules, and resource allocation to improve efficiency and reduce costs [16, 28, 29]. In manufacturing, they are used for process optimization, quality control, and supply

chain management, enhancing productivity and competitiveness [15, 16, 30].

Generally, we categorize metaheuristics into Swarm Intelligence (SI) algorithms, Physics-based Algorithms (PhA), Evolutionary Algorithms (EA), and Human-based algorithms. Swarm Intelligence (SI) algorithms are the most prototypical among the four categories [21, 31]. SI algorithms are inspired by the collective behavior observed in nature, particularly among social insects like ants and wolves. These algorithms utilize simple rules followed by the population to search for efficient solutions to optimization problems [32]. SI algorithms have the advantages of a simple structure, straightforward implementation, and self-learning behavior. These advantages enable us to find good solutions in a reasonable time frame, combined with their flexibility [33]. For instance, M. Dorigo, M. Birattari, and T. Stutzle introduced Ant Colony Optimization (ACO), which mimics how ants identify the best paths between their colony and food sources and back by leaving and following pheromones [34]. In this process, ants leave pheromone trails that help other ants to the food source. Shorter paths accumulate more pheromones and thus become more attractive. This method can be applied to various optimization tasks, such as network routing and logistics [31]. J. Kennedy and R. Eberhart introduced Particle Swarm Optimization (PSO), which draws inspiration from the flocking behavior of birds and the schooling behavior of fish [21]. In PSO, a population of candidate solutions, namely particles, moves around the search space influenced by their own best-known positions and the best-known positions of their neighbors. This approach mimics social interaction and information sharing among individuals, leading to efficient exploration and exploitation of the search space [35]. Both algorithms are simple and flexible, as they are easy to implement and can be adapted to a variety of optimization tasks such as network planning and engineering design [36]. It also inspires more and more novel SI-based optimization algorithms with a reasonable computational resource, a great searching ability, and effective improvement [37].

The No Free Lunch theorem tells us that no single algorithm can deal with all types of complex optimization problems [38]. This fundamental principle highlights the inherent limitations of any single optimization technique. In simple terms, one algorithm may have excellent optimization performance in one set of tasks but perform poorly in another [39]. This variability underscores the necessity for a diverse array of optimization algorithms tailored to specific problem domains [40]. Therefore, we introduce a novel swarm intelligence (SI) algorithm called the Dead Leaf Butterfly Optimizer (DLBO) to solve engineering industry design problems involving optimization like compression spring design, pressure vessel design, multi-disc clutch brake design, and robot gripper problems. DLBO draws inspiration from the camouflage of the dead leaf butterfly, The dead leaf butterfly protects itself in nature through its unique camouflage abilities. Its wings, both in color and shape, closely resemble dead leaves, allowing it to blend effectively into its surroundings and avoid predator attacks.

When in danger, the butterfly can also spread its wings to reveal color-changing areas on its back, which typically feature more vivid colors and patterns, creating strong visual contrast to scare off enemies. In addition, the butterfly utilizes the flexibility and positioning of its wings to enhance the camouflage effect, making it nearly undetectable when stationary. Such combination of camouflage and deterrence gives the dead leaf butterfly with a significant survival advantage in the wild, a biological phenomenon that exemplifies effective adaptation and survival strategies in nature [41]. The mathematical model of DLBO encapsulates several critical phases: initialization, exploration, development, and migration. Experiments in this paper show that the new optimizer surpasses commonly used metaheuristic algorithms, highlighting its strong application potential [42]. Through rigorous testing, DLBO has shown superior performance throughout different benchmark problems, further validating its effectiveness and robustness [43]. This superior performance underscores the value of continued innovation in optimization algorithm design, as it offers practical solutions to complex real-world tasks and challenges [5].

This paper aims to develop an efficient optimization algorithm to tackle real-world engineering and medical diagnosis challenges. To achieve this, we introduce the DLBO, designed to optimize engineering design tasks and enhance the efficiency of hyperparameter tuning in medical diagnosis. Firstly, to validate the application of DLBO in real-world engineering, we applied it to five typical engineering design problems: compression spring design, pressure vessel design, multi-disc clutch brake design, and robot gripper optimization. The experimental results showed that DLBO performed exceptionally well in solving various complex engineering problems.

In recent years, deep learning models have achieved significant success in various fields[44-50], with Graph Neural Networks (GNNs) being one of the groundbreaking advancements, specifically designed for processing graph-structured data. GNNs are particularly suited for handling complex data types where entities are interrelated in non-Euclidean spaces, making them widely applicable in fields like social network analysis, recommendation systems, and especially in biomedical data analysis. Among the various types of GNNs, Graph Convolutional Networks (GCNs)[51] have become the most classic model and the cornerstone of the entire field. GCNs excel at feature fusion by transmitting information between nodes and combining multiple features, allowing the model to effectively capture the relationships between different features[52-54]. This makes GCNs particularly suitable for biomedical datasets, where they can efficiently process and integrate various types of feature information. In the application to breast cancer data, we treat features as nodes and construct an adjacency matrix by calculating the correlation coefficients between features, using GCN for medical diagnosis. By fine-tuning the hyperparameters of the GCN model with the DLBO optimization algorithm, experimental results show that DLBO significantly improves the predictive accuracy of the GCN model, enhancing its ability to

perform disease classification, particularly in the classification of molecular subtypes of breast cancer. The DLBO-GCN model not only improves classification accuracy but also provides strong support for clinical decision-making by identifying subtle patterns within the dataset. By capturing the complex relationships between features in the dataset, the DLBO-GCN model offers valuable insights for precision medicine and further supports the development of personalized treatment plans.

In conclusion, this study not only validates the advantages of the DLBO algorithm in complex medical tasks but also showcases its broad potential in engineering design, further advancing the fields of precision medicine and engineering optimization.

The remainder of this paper is structured as follows. **Section 2** describes the DLBO inspiration and mathematical model. **Section 3** introduces the results from various experiments and analyzes them in detail. **Section 4** utilizes DLBO to solve design problems in the field of engineering. **Section 5** compares the DLBO algorithm with 11 others in optimizing GCN hyperparameters on the breast cancer dataset, showcasing DLBO's superior performance. The conclusion in **Section 6** highlights future research opportunities.

2. The dead leaf butterfly optimizer (DLBO)

2.1 Inspiration

Leaf Butterflies are a fascinating group of butterflies known for their extraordinary ability to mimic leaves, making them masters of camouflage. The most famous of these butterflies is the Dead Leaf Butterfly (Kallima inachus), but there are several other species within the Kallima genus and related groups that display similar leaf-like camouflage. The DLBO algorithm is inspired by the adaptive color-changing behavior of dead leaf butterflies in their natural environment, and it achieves optimization in dynamic conditions by simulating their different stages of color change [55-57]. **Fig. 1** shows the appearance of the butterfly. The upper side of the wings displays vibrant colors, typically featuring shades of blue, orange, and black, which become visible when the butterfly takes flight [56, 58]. In contrast, the underside of the wings imitates a dead leaf, complete with realistic spots and markings [57, 59, 60]. With its excellent camouflage ability as a defense mechanism against predators, these butterflies thrive in forests and wooded areas where they can easily blend in with the leaf litter on the forest floor by closing their wings when resting on trees and shrubs [25, 60]. The butterfly also enhances its camouflage by adopting behaviors that mimic the natural movements of leaves [9, 25]. For example, it may

sway slightly as if moved by the wind, adding to the illusion that it is just another leaf [58, 61]. In some cases, the butterfly's coloration and patterns may change slightly with the seasons, enhancing its ability to blend in with the varying types of leaf litter present at different times of the year [59, 62]. The exploration mechanisms are inspired by the different discoloration behaviors of the dead leaf butterfly when facing different scenarios [18, 55].

Besides its camouflage, its agility also plays an important role in escaping from predators. When disturbed, the butterfly employs a sudden burst of rapid flight. During this flight, it often reveals the bright, contrasting colors on the inner surfaces of its wings. This sudden flash of color can startle predators, providing the butterfly with an opportunity to escape [19, 63, 64]. This instinct of escaping gives us the inspiration of the mechanism which can avoid common optimization pitfalls like local optima trapping [61, 65]. In general, the Dead Leaf Butterfly explores the best color to display and escape to other locations with the help of camouflage to survive within the forests [9, 21]. Inspired by this, a new metaheuristic algorithm DLBO is introduced. Next, we will include some detailed explanations of the mathematical model related to such processes [17, 18, 66].

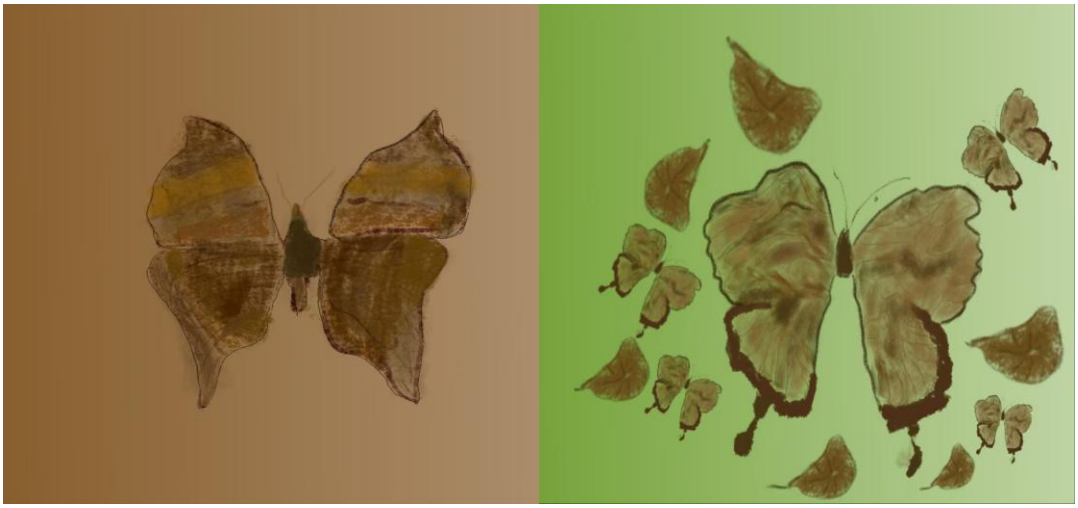

Fig. 1. The dead leaf butterfly.

2.2 Population initialization

As in most algorithms, DLBO candidate solutions are generated through Equation 1. The equation is randomly generated within the given constraints and requires update after every iteration.

$$X_i = lb + (ub - lb) \cdot rand(1, dim), \quad i = 1,2, \dots, N \tag{1}$$

where, X denotes the position of each dead leaf butterfly agent and a candidate solution, N represents the population size, and dim denotes the dimension of the problem and ub and lb are the upper and lower bounds of the problem, respectively, and rand(1, dim) is a vector of dimension dim, where each dimension is generated by a uniformly distributed random number between 0 and 1..

Fig. 2. The behavior of the dead leaf butterflies' camouflage.

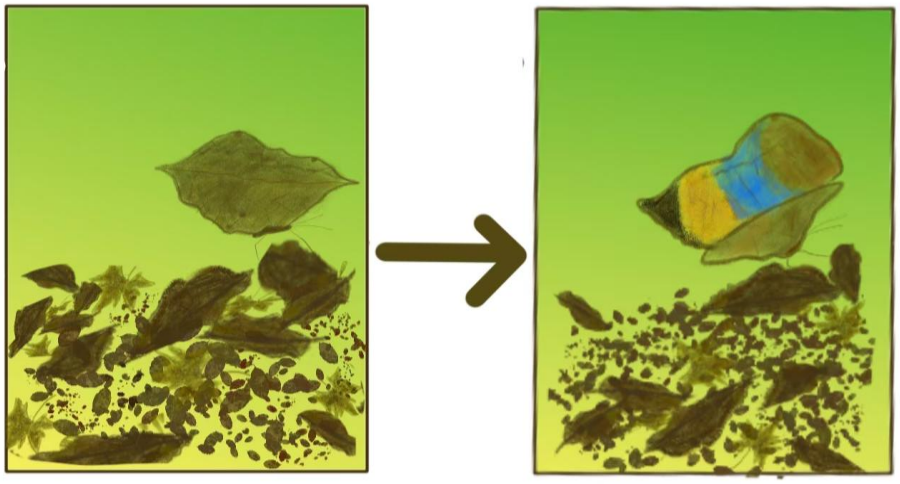

Fig. 3. The behavior of the dead leaf butterflies' mimic discoloration.

2.3 Exploration phase in the process of the dead leaf butterflies' discoloration and camouflage

In DLBO, the camouflage and discoloration abilities of dead leaf butterflies are abstracted into exploration strategies in the algorithm. These strategies embody how dead leaf butterflies use their environment for camouflage to adapt to different survival challenges, including escaping predators and finding resources. These strategies are based on the behavior of dead leaf butterflies in their natural environment, and mainly include three color-changing behaviors to enhance the exploration ability and diversity of the algorithm. dead leaf butterflies change their appearance to match their surroundings in order to avoid detection by predators. In the algorithm, this behavior is simulated as the following three strategies:

- **Collective discoloration** (shown in **Fig. 2**): In nature, the butterfly adapts to its environment by moving toward locations that enhance its camouflage. In DLBO, each individual is attracted towards the current global best solution, represented by the following equation:

$$X_i^{t+1} = X_i^t + \alpha \cdot (X_{best}^t - X_i^t) + \varepsilon \tag{2}$$

where， X_i^t is the position of individual i at iteration t. X_{best}^t is the global best position found. $\alpha = \frac{\mathcal{N}(0,1)}{10}$ is a random step size, representing the butterfly's adaptive movement towards a more camouflaged position,$\varepsilon = \frac{\mathcal{N}(0,1)}{10}$represents a slight disturbance when the dead leaf butterfly moves. $\mathcal{N}(0,1)$ represents a normally distributed random variable with a mean of 0 and a variance of 1. This behavior reflects how the butterfly optimizes its position based on the collective knowledge of the population.

- **Mimic discoloration**: The individual mimics the positions of the others, especially the ones with better performance

$$X_i^{t+1} = X_i^t + \beta \cdot \left(X_j^t - X_i^t\right) + \varepsilon \tag{3}$$

where, X_j^t is the position of a randomly selected, better performing individual. β is the step size governing the degree of mimicry,generated by a uniform distribution of the interval [0,1]. This formula mimics the butterfly's ability to learn from others' successes, helping it adapt to dynamic environments.

- **Recollective discoloration**: The individual recollects and tries to return to its historical optimal position.

$$X_i^{t+1} = X_i^t + \gamma \cdot \left(X_i^p - X_i^t\right) + \varepsilon \tag{4}$$

where, X_i^p is the historical best position of individual i. $\gamma = \frac{\mathcal{N}(0,1)}{10}$ is the step size that determines how much the individual returns to its best-known position. This behavior corresponds to the butterfly recollecting and returning to a previously effective camouflage position.

2.4 Exploitation phase of the dead leaf butterflies' protective color strategy

In the Exploitation phase, as shown in **Fig. 3**, the DLBO algorithm mimics the protective color strategy of the dead leaf butterfly, conducting deeper searches to find currently known high quality solutions. At this stage, each individual primarily optimizes its position by using comprehensive exploration behavior, that is, attempting to integrate information about the global best, the individual's historical best, and the nearest individual. In this way, the algorithm not only mimics the strategy of dead leaf butterflies to hide themselves from predators by changing color in their natural environment, but also takes advantage of their ability to locate the safest spot in space.

$$X_i^{t+1} = X_i^t + \frac{1}{3}\left(\delta_1 \cdot (X_{best}^t - X_i^t) + \delta_2 \cdot \left(X_i^p - X_i^t\right) + \delta_3 \cdot (X_{near}^t - X_i^t)\right) + \varepsilon \tag{5}$$

where, δ_1 and δ_2 are random weights representing the influence of the global best, personal best, and nearest neighbor, respectively. X_{near}^t is the position of the nearest neighbor to individual i. This behavior simulates how butterflies may combine information from multiple sources (global position, personal experience, and local surroundings) to optimize their position.

2.5 Migration Behavior of the dead leaf butterflies

In the optimization process, when individuals fail to find better solutions than the current global best over several iterations, the algorithm may become trapped in a local optimum. To avoid this issue, DLBO incorporates migration behavior. This behavior simulates the sudden flight of the Dead Leaf Butterfly when threatened, allowing individuals to escape local optima and explore new areas of the search space.

- **Migration trigger condition**: The migration behavior is triggered when the global best solution does not significantly improve for a number of iterations. Let the stagnation counter be *d*, and the threshold for triggering migration be N_s Migration is initiated when:

$$d \geq N_s \tag{6}$$

- **Migration update rule**: Once migration is triggered, a portion of the population is relocated based on the current global best solution X_{best}^t and a randomly generated migration target. The migration target position is determined by the following equation:

$$X_m = X_{best}^t + \epsilon \cdot (U - L) \tag{7}$$

where $\varepsilon = \frac{\mathcal{N}(0,1)}{10}$ and U and L are the upper and lower bounds of the search space, respectively.

- **Selection of migrating individuals**: A portion of the population is selected to participate in the migration. Given the population size *N*, the number of migrating individuals N_m is determined by the migration ratio θ as follows:

$$N_m = \theta \cdot (N - 1) \tag{8}$$

$$X_i^{t+1} = X_i^t + rand(1, dim) \cdot (X_m - X_i^t) \tag{9}$$

where η controls the step size for migration, and $X_{migration}$ is the computed migration target position.

The primary purpose of migration behavior is to help individuals escape local optima, thereby increasing the diversity of the population and preventing premature convergence. By introducing a random migration target and relocating a portion of the individuals, DLBO can explore new potential global optima in the search space. **Algoritm 1** and **Fig. 4** show the pseudo-code and flowchart of DLBO respectively

Algorithm 1 Dead Leaf Butterfly Optimization (DLBO)

1: Begin
2: Initialize the population ***X, t=0, d=0***
3: Generate the solutions' initial positions randomly
4. **While** *t*<=*T*
5. Calculate $p_1 = 1 - \frac{t}{T}$
6. Calculate $p_2 = 0.2 + 0.3 \cdot \frac{t}{T}$
7. Calculate $p_3 = 0.8 - 0.3 \cdot cos\left(\frac{\pi}{2} \cdot \frac{t}{T}\right)$
8. **If** $r_1 < p_1$:
9. **If** $r_2 < p_2$
10. Perform Collective discoloration with ***Eq (2)***
11. **End if**
12. **If** *r* < *0.5*
13. Perform Mimic Color Change with ***Eq (3)***
14. **End if**
15. **If** $r < p_3$
16. Perform Recollective discoloration Color Change with ***Eq (4)***
17. **End**
18. **Else**
19. Perform protective color strategy with ***Eq (5)***
20. **End if**
21. Update best fitness $\boldsymbol{f_{best}}$, best solution $\boldsymbol{X_{best}}$, The historical optimum $\boldsymbol{X_i^p}$ of each individual $\boldsymbol{X_i}$
22. ***If*** the current best fitness has not been improved and *d*>=N_s

23. Perform Migration Behavior with ***Eq (7)-Eq (9)***

24. ***d=0***

25. ***Else***

26. ***d=d+1***

27. ***End If***

28. t=t+1

26**End While**

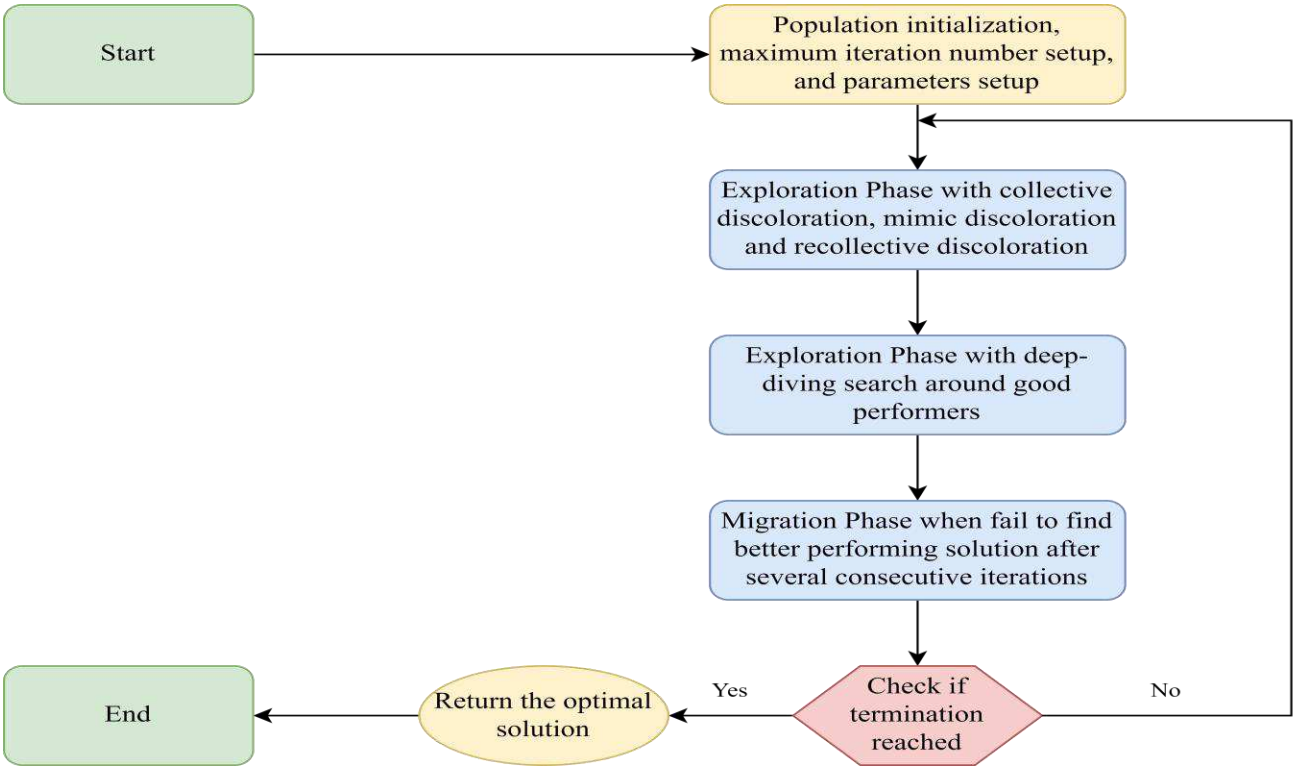

Fig. 4. The flow chart of dead leaf butterfly optimizer.

3. Numerical Experiment

In this section, we mainly assess the DLBO performance on different function test suites. To verify the competence of DLBO, we conducted convergence behavior testing. Next, we also compare the numerical experimental results of DLBO with other state-of-the-art algorithms. In addition to the effectiveness, we also demonstrate the scalability of the algorithm by applying the optimizer to large-scale tasks. All outcomes from the experiments are included in the following subsections.

3.1 Benchmark test functions

The benchmark test function is essential to evaluate the viability of the algorithm being tested. In simple words, it works as a scale to compare various optimization algorithms. In this study, we utilize both the CEC2017 and the CEC2022 test suites to assess the effectiveness of the newly introduced DLBO, setting the dimensions to 10, 20 in CEC2022 and 30, 50, and 100 in CEC2017 respectively. The optimization problem becomes more and more challenging as the dimension rises due to the increasing number of local optima. Hence, the test suites provide one of the most straight-forward ways to quantitatively analyze the performance of the algorithm. Detailed information regarding the CEC2017 test suite is attached in **Table 1**. CEC2017 suites contains four types of functions: Unimodal, Multimodal, Hybrid, and Composition functions, all of which confirm the algorithm's proficiency in local exploitation and global search.

Table l CEC2017 benchmark functions

CEC2017 Benchmark Functions			
Type	No.	Functions Description	F_t^*
Unimodal Functions	F1	Shifted and Rotated Bent Cigar Function	100
	F2	Shifted and Rotated Sum of Different Power Function	200
	F3	Shifted and Rotated Zakharov Function	300
Simple Multimodal Functions	F4	Shifted and Rotated Rosenbrock's Function	400
	F5	Shifted and Rotated Rastrigin's Function	500
	F6	Shifted and Rotated Expanded Scaffer's F6 Funetion	600
	F7	Shifted and Rotated Lunacek Bi_Rastrigin Function	700
	F8	Shifted and Rotated Non-Continuous Rastrigin's Function	800
	F9	Shifted and Rotated Levy Function	900
	F10	Shifted and Rotated Schwefel's Function	1000
Hybrid Functions	F11	Hybrid Function l (N=3)	1100
	F12	Hybrid Function 2 (N=3)	1200
	F13	Hybrid Function 3 (N=3)	1300
	F14	Hybrid Function 4 (N=3)	1400
	F15	Hybrid Function 5 (N=3)	1500
	F16	Hybrid Function 6 (N=3)	1600
	F17	Hybrid Function 6 (N=3)	1700
	F18	Hybrid Function 6 (N=3)	1800
	F19	Hybrid Function 6 (N=3)	1900
	F20	Hybrid Function 6 (N=3)	2000
Composition Functions	F21	Composition Function 1(N=3)	2100
	F22	Composition Function 2(N=3)	2200
	F23	Composition Function 3(N=3)	2300
	F24	Composition Function 4(N=3)	2400
	F25	Composition Function 5(N=3)	2500

F26	Composition Function 6(N=3)	2600
F27	Composition Function 7(N=3)	2700
F28	Composition Function 8(N=3)	2800
F29	Composition Function 9(N=3)	2900
F30	Composition Function 10(N=3)	3000

Search Range: $[-100,100]^D$

*Please Note: These problems should be treated as black-box problems. The explicit-equations of the problems are not to be used.

Table 2 CEC 2022 benchmark functions

CEC2022 Benchmark Functions			
Type	No.	Functions Description	F_t^*
Unimodal Function	1	Shifted and full Rotated Zakharov Function	300
Basic Functions	2	Shifted and full Rotated Rosenbrock's Function	400
	3	Shifted and full Rotated Expanded Schaffer's f6 Function	600
	4	Shifted and full Rotated Non-Continuous Rastrigin's Function	800
	5	Shifted and full Rotated Levy Function	900
Hybrid Functions	6	Hybrid Function 1 (N= 3)	1800
	7	Hybrid Function 2 (N= 6)	200
	8	Hybrid Function 3 (N= 5)	2200
Composition Functions	9	Composition Function 1 (N=5)	2300
	10	Composition Function 2 (N=4)	2400
	11	Composition Function 3 (N=5)	2600
	12	Composition Function 4(N=6)	2700

Search range: $[-100, 100]^p$

*Please Note: These problems should be treated as black-box problems. The explicit equations of the problems are not to be used.

3.2 Competitor algorithms and parameters setting

We compare the performance of DLBO with 11 state-of-the-art algorithms, including MELGWO [67], HSCA [68], GQPSO [69], WOA [64], GSA [70], MFO [71], SCHO [61], PO [72], NRBO [73], CPO [74], and HO [75],because these algorithms are recognized for their effectiveness in solving complex optimization problems. MELGWO and HSCA are known for their high convergence speed, while GQPSO and WOA excel in exploring the search space. GSA and MFO provide foundational insights into classical methods, and SCHO, PO, NRBO, CPO, and HO incorporate innovative strategies for improved efficiency. This diverse selection ensures a comprehensive evaluation of DLBO's performance. **Table 3** includes the parameters of the listed

competitors. The maximum number of iterations is set to and the size of the population is set to 30. We also conduct independent runs for all 12 algorithms in this competition.

Table 3 Parameter settings

Competitors	Name of the Parameter	Value of the parameter
MELGWO	P_{min}, θ, c_1	$10, decreases\ from\ 2\ to\ 0,\ 2$
HSCA	L, β	1,0.99
GQPSO	w_1, w_2, c_1, c_2	0.5,1,1.5,1.5
WOA	a, b	$decreased\ from\ 2\ to\ 0,2$
GSA	$G_0,$	100,20
MFO	b, r	$1, linear\ reduction\ -1\ to\ -2$
SCHO	$ct, u, m, \varepsilon, n, \alpha, \beta, p, q$	3.6,0.388,0.45,0.003,0.5,4.6,1.55,10,9
PO	$C_1, C_2, \mu,$	0.2,3,25,3
NRBO	p, q, CF, ε	$[2,5], [10, n], [0,1], 0.5$
CPO	N, a, N_{min}, Tf, T	120,0.1,80,0.5,2
HO	α	0.05
DLBO	$\theta, \mathrm{N_s}$	0.2,3

3.3 Convergence behavior evaluation

In order to examine whether DLBO is convergent or not, in **Fig. 5**, we set up experiments to investigate the convergence behavior of the algorithm. As shown in Fig., the first column displays the 3-D parameter space of the function, which is a straightforward illustration of the complexity of the problem. The second column demonstrates the search trajectories of the search agent. The search trajectory refers to the path or sequence of points that an algorithm visits in the solution space while searching for the optimal solution. Understanding and analyzing search trajectories helps in designing more efficient algorithms, balancing exploration and exploitation, and avoiding common pitfalls like premature convergence and local optima trapping. The third column showcases the change in the average fitness value of each search agent as the number of iterations increases. The fitness value in optimization algorithms is a measure of how well a candidate solution performs relative to other solutions in the context of the problem being solved. It serves as a quantitative evaluation of a solution's quality, guiding the search process toward optimal or near-optimal solutions. DLBO consistently achieves a low fitness

value within the maximum number of iterations, demonstrating its strong ability to find the global optimal solution. The fourth column shows the search trajectory during the process, which clearly trends toward stability. The last column shows the convergence curve of DLBO. From the chart, we can see that generally DLBO can converge within 400 iterations. From the curve, we can see that DLBO is able to obtain the global optimum within all kinds of functions in the suite. The rapid convergence speed indicates that DLBO can arrive at global optimum with a reasonable computational resource. Overall, we conclude that DLBO is convergent and can be applied to tackle various tasks within a suitable time frame.

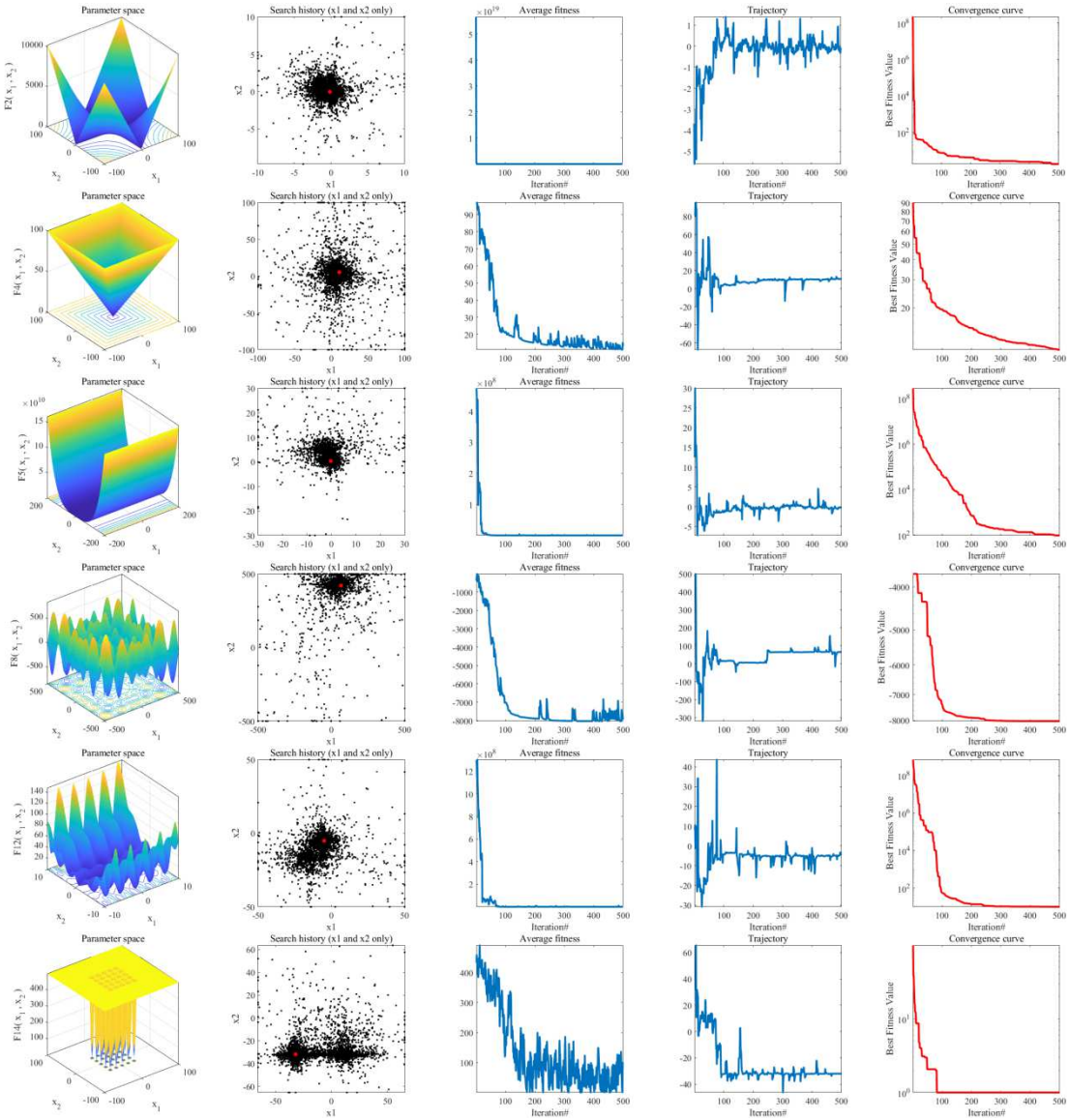

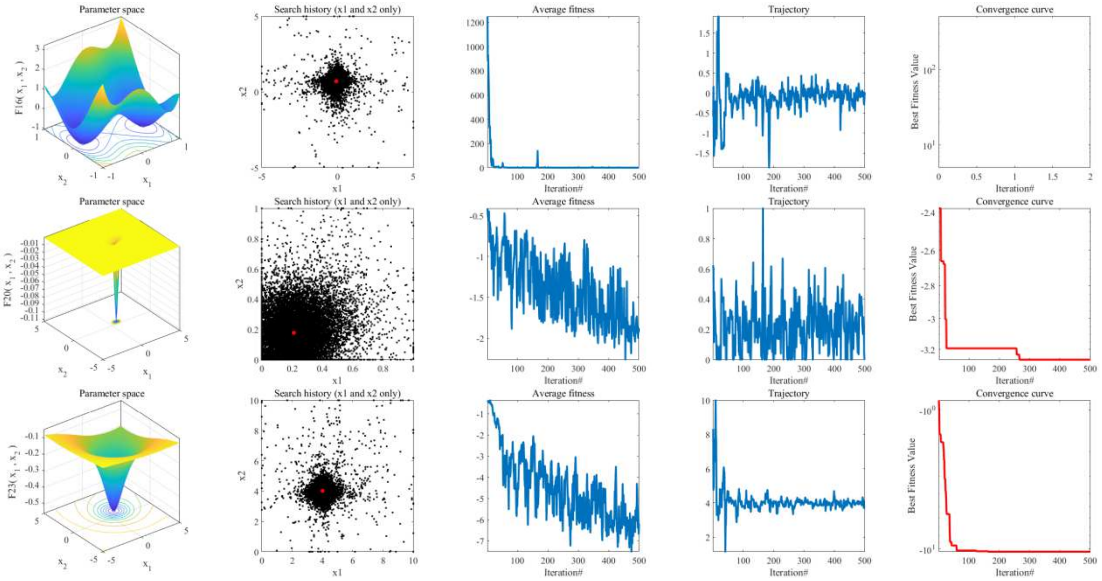

Fig. 5. Convergence behaviors of DLBO in the search process.

3.4 Quantitative analysis

In this section, we review the numerical optimization performance of the different competitors using CEC2017 and CEC2022 test suites.

3.4.1 Comparison with other competitive algorithms on CEC2022

In this section, we utilize the Sankey diagram from the CEC 2022 benchmark suite for performance testing, setting the problem dimensions to 10 and 20, respectively. To visualize the ranking distribution of each algorithm, the experimental results, including the mean value (Ave) and standard deviation (Std), are detailed in **Tables 4** and **Table 5**. **Fig. 6** presents a comparative ranking analysis of the DLBO algorithm against various other algorithms for 10-dimensional and 20-dimensional problems in the CEC 2022 benchmark tests. Particularly for the 10-dimensional problems, as shown in **Fig. 6-1**, the DLBO algorithm consistently ranks within the top four, demonstrating its stability and efficiency. In contrast, algorithms such as GQPSO and GSA exhibit more dispersed rankings, lacking the same level of consistency and high performance.

In **Fig. 6-2**, the DLBO algorithm continues to showcase its superiority, especially evident in its frequent attainment of first place, significantly outperforming other algorithms. For instance, the GQPSO algorithm, known for its advanced and popular capabilities, demonstrates notable performance; however, it does not maintain the same level of stability as the DLBO algorithm. Furthermore, algorithms like WOA and GSA display

competitive performance in certain rankings but still fall short of DLBO in terms of consistency and peak efficiency.

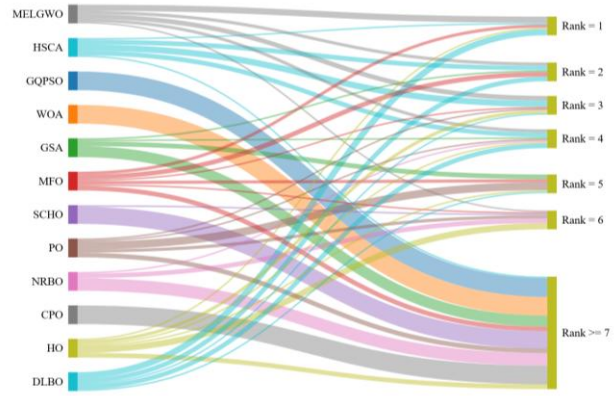

Fig. 6-1. Sankey diagram of DLBO convergence behavior

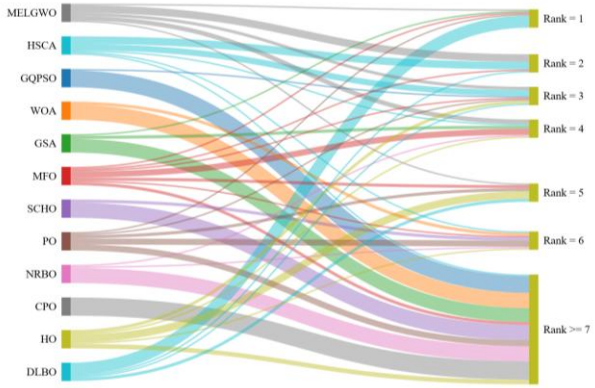

Fig. 6-2. Sankey diagram of DLBO convergence behavior

Fig. 7 reveals noticeable differences in the convergence curves of various algorithms for 10-dimensional and 20-dimensional problems. For 10-dimensional issues, most algorithms improve performance as the number of iterations increases, with the DLBO algorithm demonstrating relatively faster convergence, particularly in the later stages of iteration, showing better stability and optimization capabilities. In 20-dimensional problems, DLBO also exhibits rapid convergence capabilities. Compared to other algorithms like MELGWO and GQPSO, DLBO continues to maintain lower objective function values in the later stages of iteration, demonstrating its effectiveness in handling high-dimensional challenges.

Fig. 8 provides further statistical analysis of algorithm performance through box plots. Across the 10-dimensional and 20-dimensional problems, the performance differences between algorithms are visually evident through the box plots' median, quartiles, and outliers. For instance, DLBO performance in 20-dimensional problems is particularly notable; its box plot displays lower performance variability and a smaller quartile range, indicating more stable results. In contrast, other algorithms such as CPO and SCHO exhibit greater performance variability on certain problems, which may suggest lower adaptability of these algorithms to specific challenges.

Overall, DLBO is outperforming in rapid convergence and high stability across multi-dimensional problems, which makes it an outstanding performer among various algorithms.

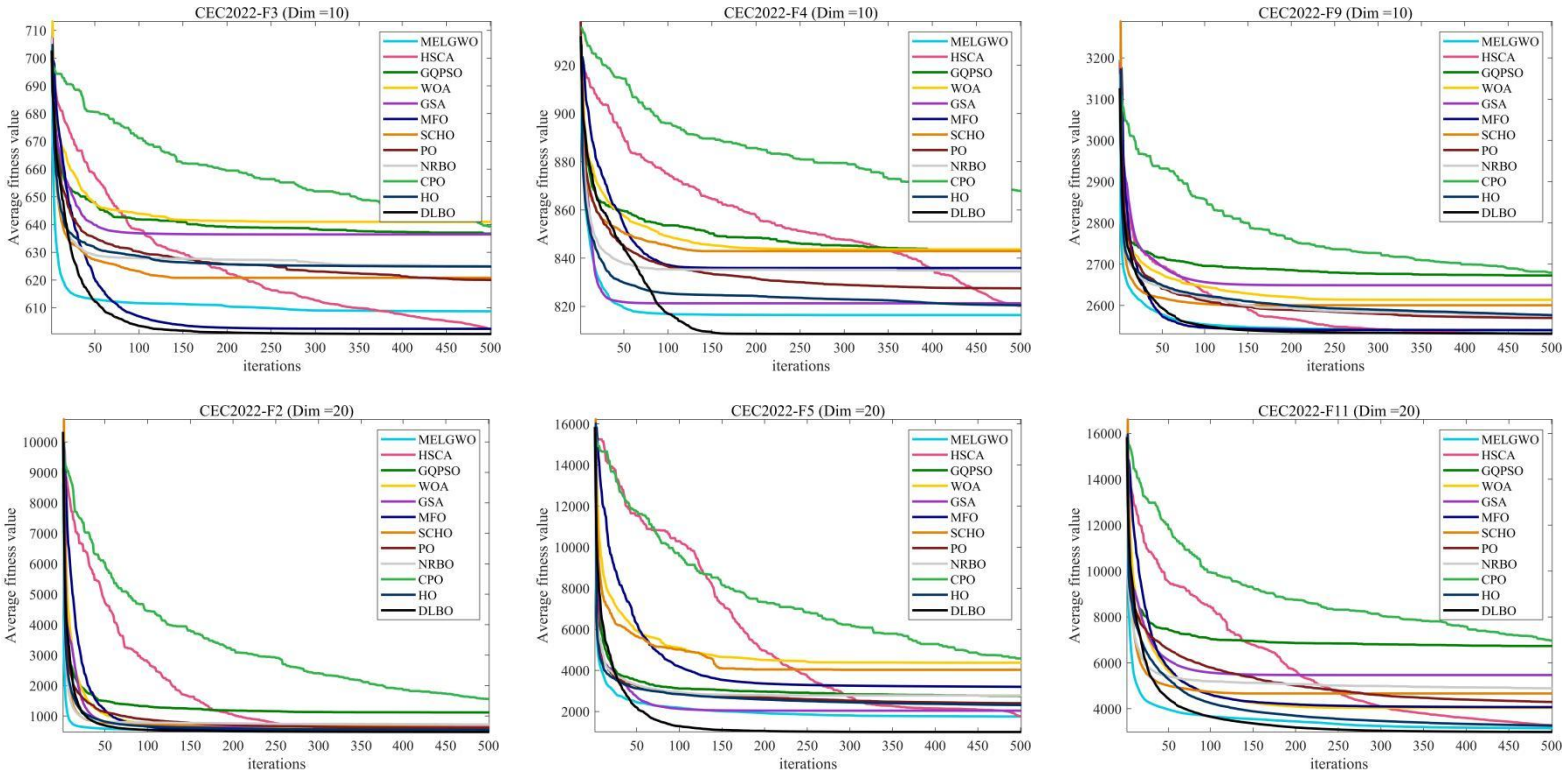

Fig. 7. Comparison of the convergence speed of different competitors on CEC2022 test suites.

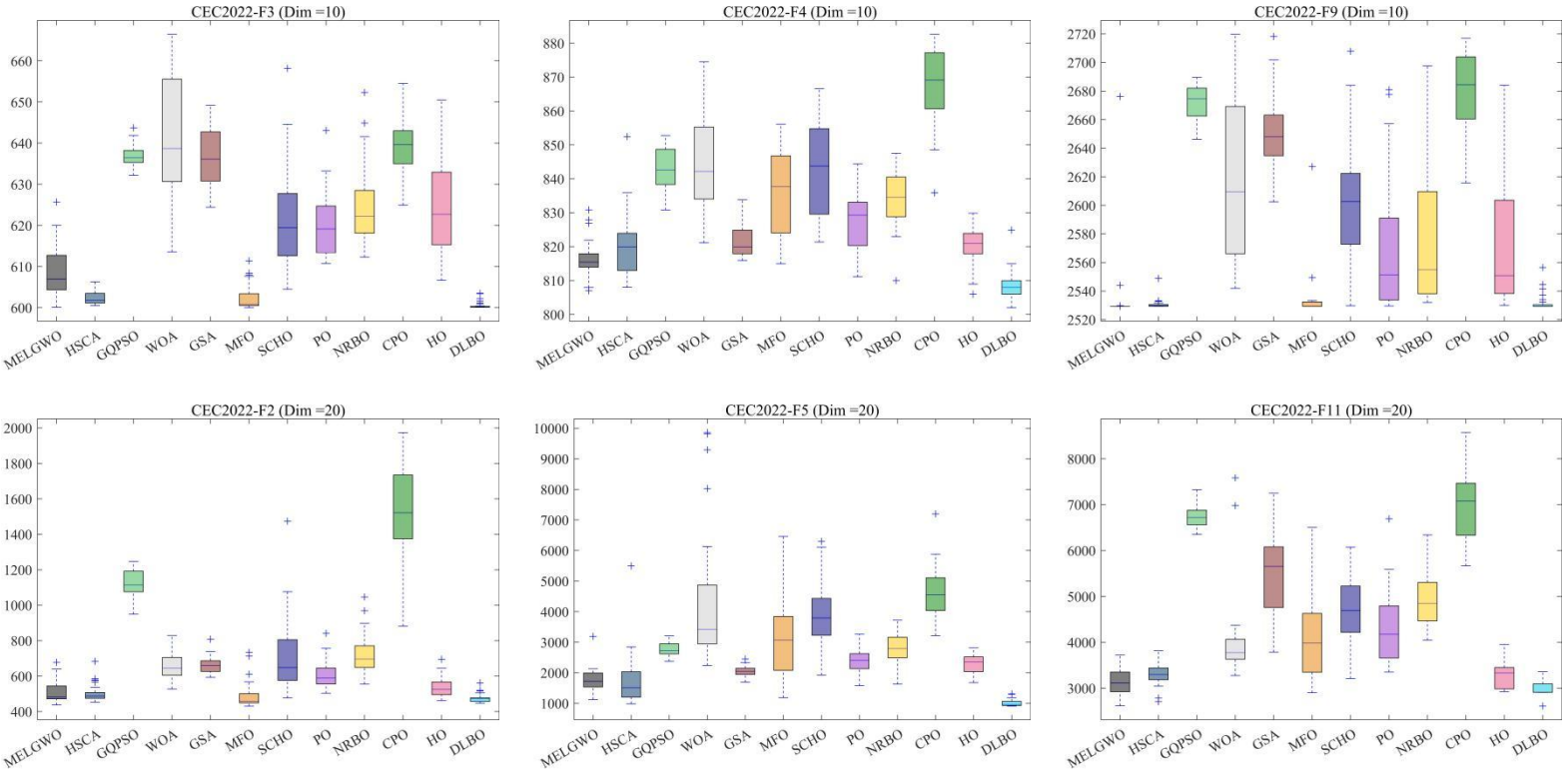

Fig. 8. Box plot of different competitors on CEC2022 test suites.

3.4.2 Comparison with other competitive algorithms on CEC2017

In this section, we conduct performance testing using the CEC 2017 benchmark suite with dimensional settings of 30, 50, and 100. To visualize the ranking distribution of various algorithms, we present the rankings of different competitors in a Sankey diagram in **Fig. 9**. **Fig. 9-1** shows that when the dimension is set to 30, the DLBO algorithm is primarily concentrated in the first position, significantly outperforming other competitors. **Fig. 9-2** indicates that at a dimension of 50, the DLBO algorithm consistently remains within the top two positions, demonstrating a remarkable performance compared to other competitors. **Fig. 9-3** illustrates that when the dimension is set to 100, the DLBO algorithm is mainly concentrated in the first position, continuing to dominate over other competitors. The experimental results are detailed in **Table 6**, **Table 7** and **Table 8**. Among the 11 participants, the best-performing results are highlighted in bold, clearly indicating that our newly developed DLBO algorithm consistently ranks within the top five, showcasing its exceptional capability. Notably, DLBO performs excellently across the 30 benchmark functions F1 to F30 in CEC 2017, achieving first place in most cases, with performance comparable to previous CEC champions. Furthermore, DLBO exhibits low sensitivity to dimensional changes. **Fig. 10** and **11** present the convergence curves of various competitors at different dimensions. To reduce the impact of random variations, the presented average iteration curves are based on 30 repeated trials. These results demonstrate that our optimizer not only converges faster but also achieves higher accuracy, clearly establishing the superiority of DLBO in this field.

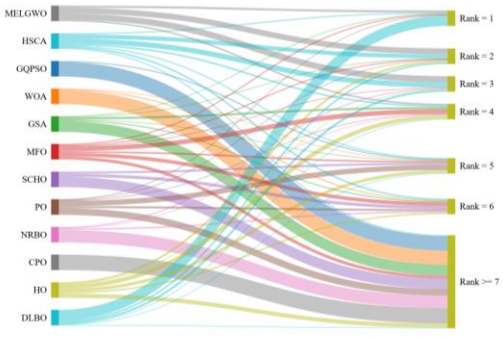

Fig. 9-1. The ranking chart of DLBO.

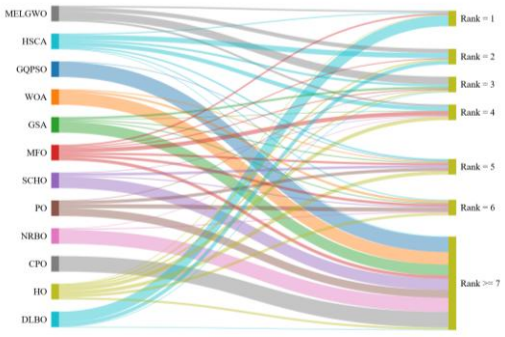

Fig. 9-2. The ranking chart of DLBO.

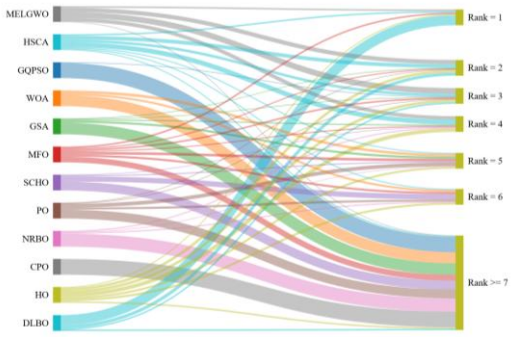

Fig. 9-3. The ranking chart of DLBO.

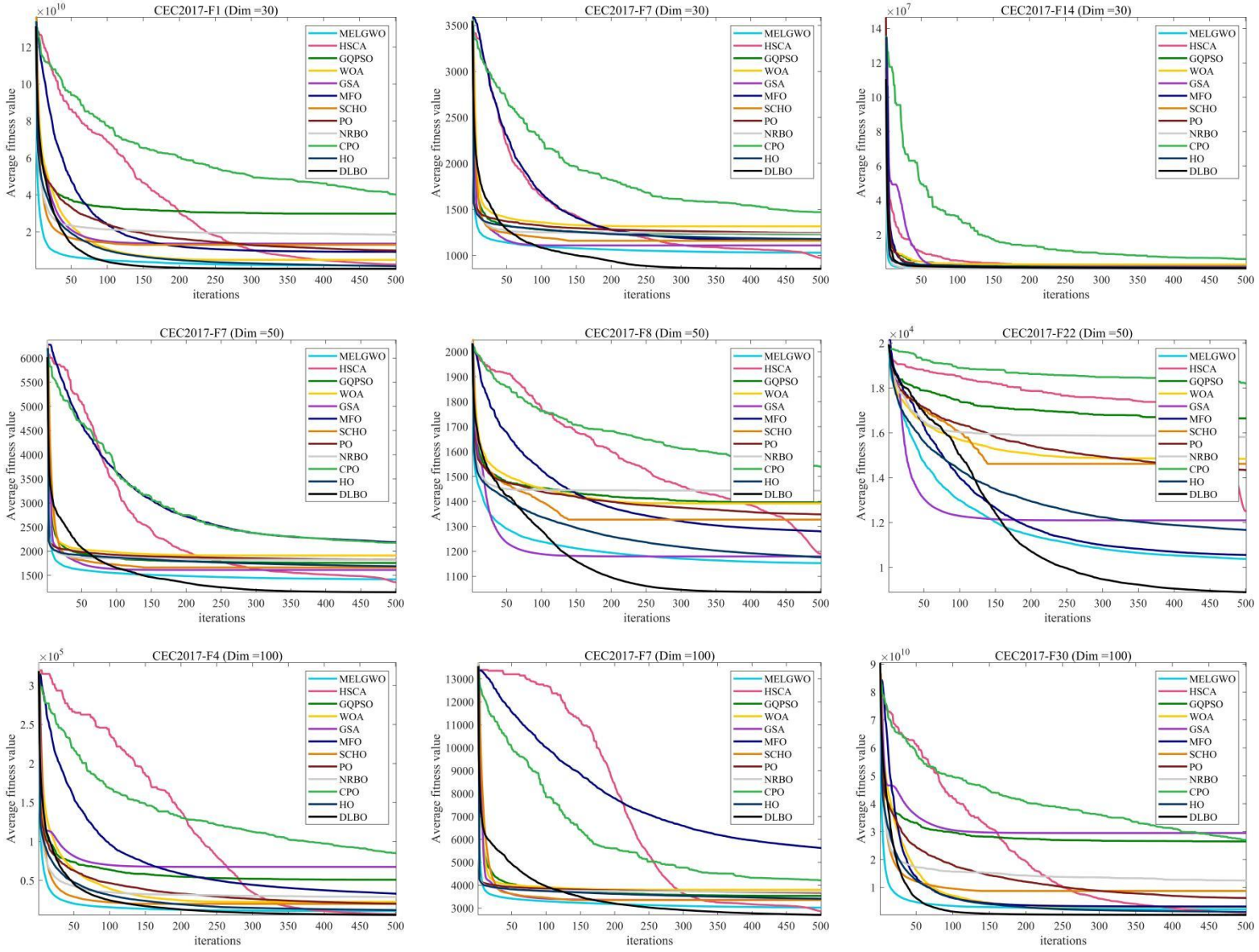

Fig. 10. Comparison of the convergence speed of different competitors on CEC2017 test suites.

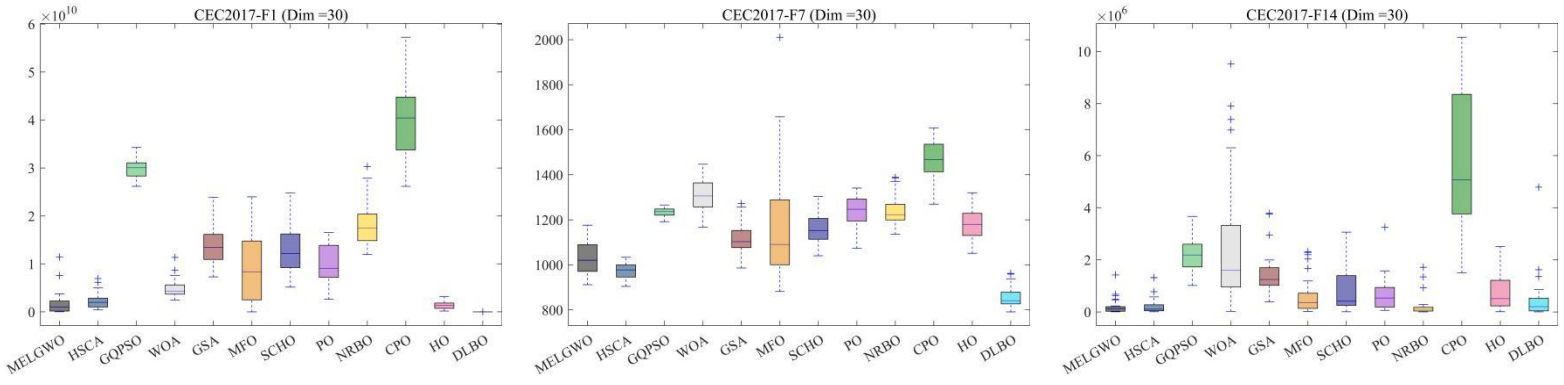

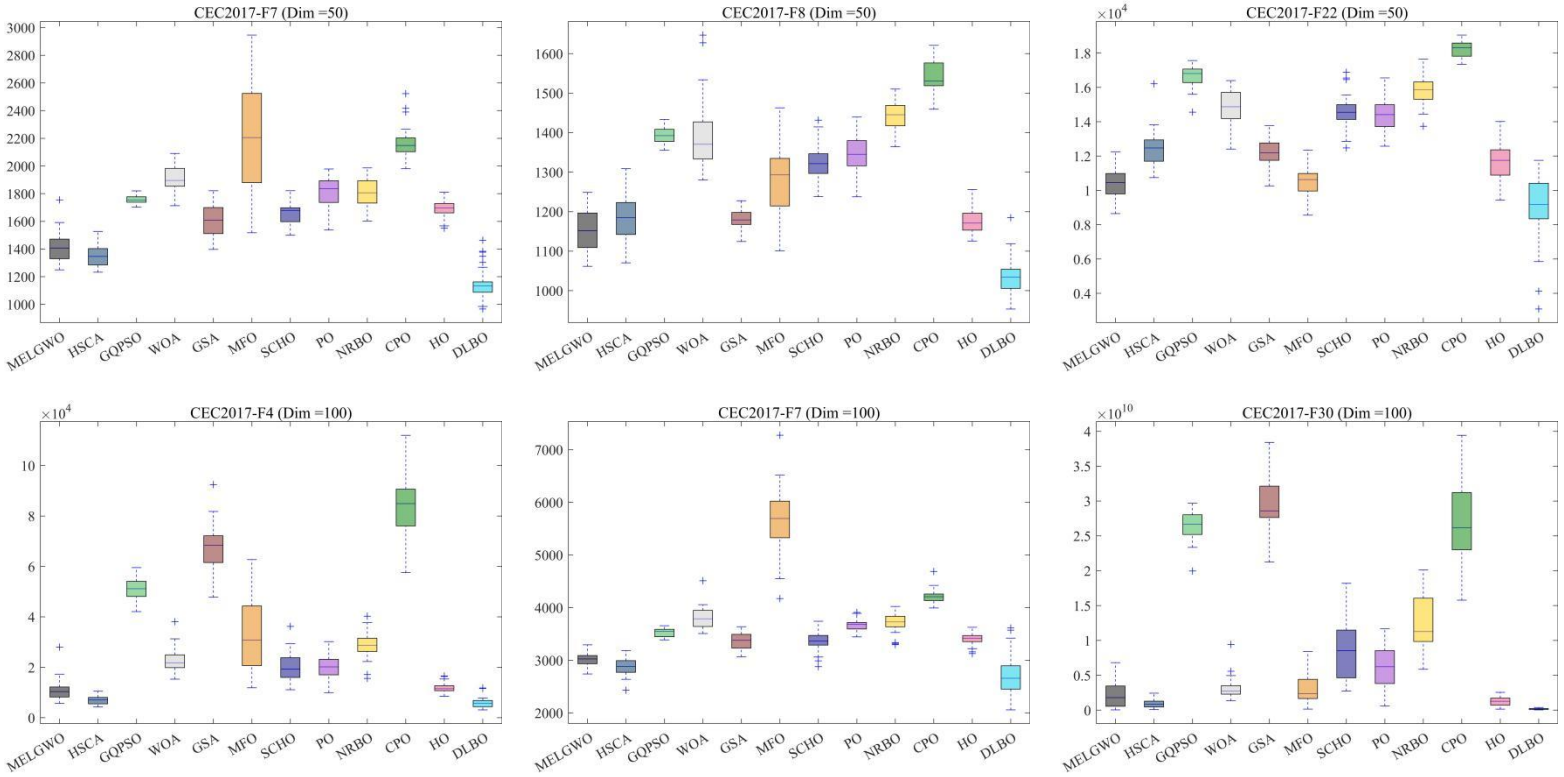

Fig. 11. Box plot of different competitors on CEC2017 test suites.

Table 4 Comparison results on CEC2022 (Dim=10).

Algorithm	Metric	MELGWO	HSCA	GQPSO	WOA	GSA	MFO	SCHO	PO	NRBO	CPO	HO	DLBO
CEC2022-F1	Avg	**3.043297E+02**	4.043478E+02	4.280546E+03	2.945021E+04	1.085597E+04	7.346160E+03	5.934902E+03	4.975097E+02	1.681082E+03	1.817177E+04	9.652266E+02	7.765852E+02
	Std	**9.788056E+00**	7.926120E+01	6.220067E+02	1.231774E+04	2.656681E+03	8.704596E+03	3.141791E+03	4.269275E+02	1.086079E+03	6.052403E+03	3.388801E+02	9.295037E+02
CEC2022-F2	Avg	4.157737E+02	**4.153851E+02**	5.889855E+02	4.952904E+02	4.378880E+02	4.172913E+02	4.832834E+02	4.450926E+02	4.553212E+02	6.874307E+02	4.417118E+02	4.199947E+02
	Std	2.561441E+01	**1.530666E+01**	2.544942E+01	1.135154E+02	4.607464E+01	2.146253E+01	9.310869E+01	3.422070E+01	2.478237E+01	1.087734E+02	3.157944E+01	2.771807E+01
CEC2022-F3	Avg	6.087402E+02	6.023703E+02	6.367350E+02	6.409747E+02	6.364376E+02	6.024161E+02	6.208114E+02	6.200306E+02	6.250830E+02	6.391832E+02	6.248667E+02	**6.005544E+02**
	Std	6.737896E+00	1.702828E+00	2.653643E+00	1.519170E+01	6.875263E+00	3.118760E+00	1.191910E+01	7.531632E+00	9.766592E+00	6.652482E+00	1.180618E+01	**9.298791E-01**
CEC2022-F4	Avg	8.164170E+02	8.202444E+02	8.431990E+02	8.436760E+02	8.212921E+02	8.359470E+02	8.429273E+02	8.275228E+02	8.345372E+02	8.679420E+02	8.204992E+02	**8.085680E+02**
	Std	5.823526E+00	9.459888E+00	6.083221E+00	1.493290E+01	4.641817E+00	1.303205E+01	1.329293E+01	8.571055E+00	8.053190E+00	1.083197E+01	5.278301E+00	**4.275330E+00**
CEC2022-F5	Avg	9.791752E+02	9.117907E+02	1.151073E+03	1.534061E+03	1.011782E+03	1.080047E+03	1.477195E+03	1.113027E+03	1.026150E+03	1.571256E+03	1.102725E+03	**9.009878E+02**
	Std	9.533493E+01	2.411966E+01	4.988555E+01	5.391544E+02	9.497351E+01	2.757881E+02	3.331825E+02	1.691034E+02	9.062064E+01	3.142887E+02	1.316114E+02	**1.922790E+00**
CEC2022-F6	Avg	3.180946E+03	6.096841E+03	5.962936E+06	5.280038E+03	2.687160E+03	5.250522E+03	2.799547E+04	4.934653E+03	3.825859E+03	3.085087E+07	**1.962933E+03**	4.026424E+03
	Std	1.488204E+03	2.161063E+03	4.241019E+06	2.299851E+03	8.106750E+02	2.294663E+03	1.846851E+04	1.937096E+03	1.858250E+03	1.743095E+07	**8.444518E+01**	1.687029E+03
CEC2022-F7	Avg	2.047505E+03	2.031030E+03	2.094650E+03	2.087610E+03	2.102807E+03	2.029792E+03	2.072962E+03	2.051778E+03	2.061716E+03	2.109920E+03	2.053269E+03	**2.028344E+03**
	Std	2.656593E+01	**8.729598E+00**	1.348720E+01	3.335096E+01	3.779556E+01	1.294246E+01	3.955939E+01	1.368326E+01	2.210391E+01	1.994783E+01	1.828151E+01	2.291841E+01
CEC2022-F8	Avg	2.223644E+03	**2.223553E+03**	2.236215E+03	2.235111E+03	2.455198E+03	2.224099E+03	2.261709E+03	2.228450E+03	2.249913E+03	2.248411E+03	2.228770E+03	2.236343E+03
	Std	3.901816E+00	6.586610E+00	3.435655E+00	1.095753E+01	1.336805E+02	**3.395776E+00**	5.333124E+01	4.938956E+00	4.612413E+01	1.105484E+01	4.510213E+00	3.800229E+01
CEC2022-F9	Avg	2.539588E+03	**2.530729E+03**	2.672551E+03	2.613450E+03	2.648981E+03	2.540291E+03	2.600408E+03	2.569700E+03	2.576971E+03	2.679242E+03	2.576333E+03	2.531778E+03
	Std	3.723679E+01	**3.569301E+00**	1.230145E+01	5.465373E+01	2.430651E+01	2.965519E+01	4.332322E+01	4.297296E+01	4.956833E+01	2.810120E+01	5.057771E+01	5.982952E+00
CEC2022-F10	Avg	2.581646E+03	**2.516735E+03**	2.552564E+03	2.642488E+03	2.758331E+03	2.572968E+03	2.658686E+03	2.530922E+03	2.584731E+03	2.562788E+03	2.546762E+03	2.558259E+03
	Std	8.651876E+01	**4.192372E+01**	6.017408E+01	2.545079E+02	3.364824E+02	2.199675E+02	2.278898E+02	5.413034E+01	6.979411E+01	7.095170E+01	6.178801E+01	5.917426E+01
CEC2022-F11	Avg	2.720697E+03	2.748149E+03	2.890334E+03	2.836299E+03	2.756550E+03	2.808778E+03	2.963804E+03	2.779526E+03	2.915939E+03	2.943457E+03	2.725404E+03	**2.714519E+03**
	Std	1.776731E+02	1.274539E+02	**4.002416E+01**	1.638934E+02	1.428899E+02	1.352984E+02	3.107971E+02	1.837790E+02	2.288837E+02	1.399336E+02	1.646079E+02	1.505646E+02
CEC2022-F12	Avg	2.868068E+03	2.864011E+03	2.958989E+03	2.903418E+03	3.105784E+03	**2.864002E+03**	2.919368E+03	2.871116E+03	2.877580E+03	2.962638E+03	2.886609E+03	2.868610E+03
	Std	1.252871E+01	**1.784683E+00**	1.249084E+01	3.719257E+01	8.760625E+01	2.136404E+00	3.608285E+01	1.298984E+01	3.003280E+01	2.831299E+01	2.475099E+01	8.785752E+00

Table 5 Comparison results on CEC2022 (Dim=20).

Algorithm	Metric	MELGWO	HSCA	GQPSO	WOA	GSA	MFO	SCHO	PO	NRBO	CPO	HO	DLBO

CEC2022-F1	Avg	**5.362555E+03**	1.377484E+04	2.366949E+04	3.806856E+04	3.057518E+04	5.133578E+04	2.101125E+04	1.432655E+04	1.493603E+04	6.212945E+04	2.351198E+04	1.998945E+04
	Std	**2.042145E+03**	5.356162E+03	3.150713E+03	1.661868E+04	5.443506E+03	2.260788E+04	7.825773E+03	4.161473E+03	3.607974E+03	1.895617E+04	6.199088E+03	9.247819E+03
CEC2022-F2	Avg	5.072795E+02	5.048737E+02	1.117313E+03	6.506577E+02	6.646564E+02	4.915202E+02	7.045035E+02	6.076504E+02	7.222497E+02	1.552071E+03	5.410632E+02	**4.753313E+02**
	Std	6.039347E+01	4.888280E+01	8.440975E+01	7.532043E+01	4.636248E+01	7.452783E+01	2.036726E+02	7.969825E+01	1.155851E+02	2.559916E+02	5.850637E+01	**2.550646E+01**
CEC2022-F3	Avg	6.280478E+02	6.123937E+02	6.661512E+02	6.699902E+02	6.616853E+02	6.248949E+02	6.507799E+02	6.491750E+02	6.589984E+02	6.724559E+02	6.519259E+02	**6.069445E+02**
	Std	1.039499E+01	4.738657E+00	**4.307774E+00**	1.217107E+01	5.269205E+00	1.197747E+01	1.158813E+01	1.129527E+01	9.909254E+00	1.026068E+01	8.830764E+00	5.740157E+00
CEC2022-F4	Avg	8.611705E+02	8.713477E+02	9.521364E+02	9.291010E+02	8.745222E+02	8.933394E+02	9.122778E+02	9.071197E+02	9.357221E+02	9.995333E+02	8.801152E+02	**8.391310E+02**
	Std	1.494872E+01	1.745556E+01	**8.697955E+00**	3.896733E+01	1.211356E+01	2.304446E+01	2.482131E+01	1.530709E+01	1.763462E+01	1.874978E+01	1.164412E+01	1.344206E+01
CEC2022-F5	Avg	1.754694E+03	1.764504E+03	2.755548E+03	4.373501E+03	2.041060E+03	3.202637E+03	4.030181E+03	2.404299E+03	2.779906E+03	4.571308E+03	2.315121E+03	**1.003137E+03**
	Std	3.956846E+02	8.738005E+02	2.315180E+02	2.164979E+03	1.667502E+02	1.270611E+03	1.208428E+03	3.701096E+02	5.367172E+02	8.426227E+02	2.911313E+02	**1.065334E+02**
CEC2022-F6	Avg	6.904643E+03	1.427713E+06	2.211678E+08	1.041836E+07	**3.003940E+03**	1.895032E+06	4.081593E+07	4.059695E+06	2.678201E+07	7.106557E+08	6.616563E+03	1.563041E+04
	Std	1.025797E+04	3.075069E+06	8.549623E+07	1.558041E+07	**8.710854E+02**	6.972857E+06	1.126287E+08	9.338985E+06	2.270894E+07	2.980153E+08	3.723385E+03	5.758633E+03
CEC2022-F7	Avg	2.119464E+03	2.083697E+03	2.202501E+03	2.222208E+03	2.350661E+03	2.124583E+03	2.198047E+03	2.157809E+03	2.163632E+03	2.279594E+03	2.153957E+03	**2.069800E+03**
	Std	4.278909E+01	3.619200E+01	**1.327351E+01**	7.535529E+01	9.773740E+01	6.192632E+01	9.615435E+01	4.392103E+01	4.291462E+01	5.001942E+01	2.233317E+01	2.061019E+01
CEC2022-F8	Avg	2.273592E+03	2.275199E+03	2.277548E+03	2.286415E+03	2.544267E+03	2.267335E+03	2.325986E+03	2.283167E+03	2.317926E+03	2.404637E+03	**2.245261E+03**	2.248074E+03
	Std	7.250778E+01	5.923588E+01	1.567269E+01	6.439002E+01	1.080303E+02	5.215525E+01	8.463304E+01	5.531857E+01	7.067099E+01	9.824299E+01	**1.036987E+01**	3.507165E+01
CEC2022-F9	Avg	2.499700E+03	2.492569E+03	2.802643E+03	2.594766E+03	2.732870E+03	2.516603E+03	2.580673E+03	2.568867E+03	2.624367E+03	2.845347E+03	2.565054E+03	**2.487948E+03**
	Std	1.360504E+01	9.361177E+00	3.744480E+01	4.576653E+01	5.377797E+01	5.494034E+01	5.468111E+01	5.651634E+01	6.422019E+01	1.073385E+02	3.664254E+01	**6.348084E+00**
CEC2022-F10	Avg	3.781847E+03	4.284525E+03	2.699522E+03	5.219253E+03	5.352979E+03	3.711666E+03	4.662943E+03	**2.687943E+03**	4.910611E+03	4.371065E+03	4.022476E+03	3.134321E+03
	Std	5.820139E+02	1.003554E+03	**1.482298E+02**	1.293194E+03	6.691077E+02	9.624600E+02	8.189777E+02	5.970789E+02	1.550227E+03	1.987348E+03	1.046981E+03	5.834033E+02
CEC2022-F11	Avg	3.152425E+03	3.287410E+03	6.735112E+03	4.040249E+03	5.468929E+03	4.071714E+03	4.666291E+03	4.296426E+03	4.894289E+03	6.974905E+03	3.261356E+03	**2.987814E+03**
	Std	2.442179E+02	2.288968E+02	2.083325E+02	9.196241E+02	8.416633E+02	9.243910E+02	7.970500E+02	7.770552E+02	5.391754E+02	7.033398E+02	2.781144E+02	**1.529869E+02**
CEC2022-F12	Avg	2.998084E+03	2.971115E+03	3.574630E+03	3.110979E+03	4.337080E+03	**2.952865E+03**	3.198847E+03	3.027563E+03	3.040143E+03	3.572871E+03	3.130474E+03	2.982531E+03
	Std	5.042468E+01	1.456836E+01	1.055481E+02	1.445268E+02	3.752121E+02	**1.199632E+01**	1.330325E+02	5.146455E+01	4.092524E+01	1.519111E+02	1.368900E+02	3.088628E+01

Table 6 Comparison results on CEC2017 (Dim=30).

Algorithm	Metric	MELGWO	HSCA	GQPSO	WOA	GSA	MFO	SCHO	PO	NRBO	CPO	HO	DLBO
CEC2017-F1	Avg	1.761336E+09	2.322895E+09	2.984067E+10	4.839859E+09	1.360751E+10	9.189920E+09	1.297034E+10	9.914296E+09	1.838600E+10	4.026213E+10	1.417468E+09	**9.531771E+05**
	Std	2.442611E+09	1.642503E+09	2.027114E+09	1.908836E+09	3.799198E+09	6.700171E+09	5.192770E+09	4.346438E+09	4.563851E+09	7.578862E+09	7.528203E+08	**2.674376E+06**

CEC2017-F2	Avg	8.220100E+31	3.142828E+29	8.290519E+38	8.132909E+36	2.347409E+50	1.835639E+43	4.757493E+43	1.402835E+35	6.553459E+35	3.137782E+43	9.688872E+32	**2.251542E+23**
	Std	3.260369E+32	1.486690E+30	1.366810E+39	2.778028E+37	1.248251E+51	1.005283E+44	2.605786E+44	7.418700E+35	1.995935E+36	1.650895E+44	3.380821E+33	**9.339467E+23**
CEC2017-F3	Avg	**4.524782E+04**	8.444190E+04	7.540906E+04	2.744593E+05	9.790016E+04	1.814939E+05	8.254120E+04	4.996931E+04	5.857242E+04	2.034197E+05	6.151510E+04	9.823497E+04
	Std	1.020522E+04	3.283067E+04	**4.825638E+03**	6.424589E+04	1.117009E+04	4.942860E+04	1.501770E+04	7.952403E+03	9.068815E+03	9.365076E+04	7.164835E+03	3.639031E+04
CEC2017-F4	Avg	6.411509E+02	6.060853E+02	5.893618E+03	1.333541E+03	3.435942E+03	1.903077E+03	1.616990E+03	1.031656E+03	2.207657E+03	8.650342E+03	7.234707E+02	**5.592861E+02**
	Std	1.584764E+02	5.919903E+01	5.399314E+02	5.286166E+02	8.872343E+02	1.374122E+03	8.369879E+02	2.340417E+02	9.201985E+02	2.003020E+03	8.605472E+01	**4.023820E+01**
CEC2017-F5	Avg	6.601067E+02	6.687876E+02	8.628160E+02	8.651837E+02	7.446997E+02	7.074013E+02	7.704861E+02	7.871081E+02	8.362415E+02	9.112424E+02	7.354179E+02	**6.082099E+02**
	Std	3.433879E+01	2.990700E+01	**1.554352E+01**	5.716355E+01	2.873602E+01	5.996582E+01	3.923533E+01	3.813856E+01	4.532182E+01	3.141823E+01	3.350756E+01	2.455415E+01
CEC2017-F6	Avg	6.414236E+02	6.243735E+02	6.753078E+02	6.817011E+02	6.622444E+02	6.421618E+02	6.607868E+02	6.663334E+02	6.719400E+02	6.837579E+02	6.643160E+02	**6.206509E+02**
	Std	9.309660E+00	7.312561E+00	**4.507161E+00**	1.304086E+01	4.869697E+00	9.595176E+00	1.069410E+01	9.666223E+00	9.097315E+00	7.848460E+00	7.519110E+00	8.133682E+00
CEC2017-F7	Avg	1.030023E+03	9.721231E+02	1.232788E+03	1.317095E+03	1.109418E+03	1.160761E+03	1.160290E+03	1.245178E+03	1.239238E+03	1.471094E+03	1.179121E+03	**8.557801E+02**
	Std	7.423682E+01	3.657558E+01	**2.100072E+01**	7.505579E+01	6.799123E+01	2.523481E+02	6.805803E+01	6.708790E+01	7.153144E+01	8.736429E+01	6.374300E+01	4.309949E+01
CEC2017-F8	Avg	9.296424E+02	9.509147E+02	1.092139E+03	1.064688E+03	9.649586E+02	1.007552E+03	1.010330E+03	1.028334E+03	1.079650E+03	1.165851E+03	9.702364E+02	**8.886882E+02**
	Std	3.333557E+01	2.952619E+01	**1.506101E+01**	4.854092E+01	1.998387E+01	5.105392E+01	3.547420E+01	3.063062E+01	2.865839E+01	2.462351E+01	2.291737E+01	2.521261E+01
CEC2017-F9	Avg	3.815493E+03	4.378137E+03	8.719405E+03	1.117379E+04	4.857837E+03	7.319400E+03	1.110451E+04	7.153224E+03	7.498393E+03	1.400710E+04	5.990294E+03	**1.607584E+03**
	Std	8.106604E+02	1.173164E+03	6.743593E+02	3.086479E+03	5.573848E+02	1.985207E+03	3.563646E+03	9.612571E+02	1.628877E+03	3.018243E+03	7.107255E+02	**4.345379E+02**
CEC2017-F10	Avg	5.273053E+03	5.961181E+03	8.723063E+03	7.722022E+03	5.321741E+03	5.544644E+03	6.906662E+03	7.151643E+03	7.952243E+03	9.628587E+03	5.396930E+03	**4.474941E+03**
	Std	6.837383E+02	7.659381E+02	**3.772626E+02**	5.619353E+02	6.136398E+02	7.660195E+02	7.135655E+02	7.725594E+02	7.119061E+02	4.739912E+02	7.784251E+02	6.396266E+02
CEC2017-F11	Avg	1.585010E+03	1.463424E+03	5.081302E+03	8.974157E+03	7.623063E+03	3.986439E+03	4.139296E+03	2.007390E+03	2.647104E+03	1.286904E+04	1.795845E+03	**1.457104E+03**
	Std	6.069895E+02	**1.208403E+02**	5.662843E+02	3.362671E+03	1.774195E+03	3.091267E+03	1.749252E+03	4.962219E+02	7.533853E+02	3.648577E+03	2.027209E+02	1.702320E+02
CEC2017-F12	Avg	1.104055E+08	8.543576E+07	7.195353E+09	5.154205E+08	2.401679E+09	3.026410E+08	1.531424E+09	3.880627E+08	1.711468E+09	6.220412E+09	2.026016E+08	**1.152495E+07**
	Std	3.289789E+08	6.363212E+07	8.181215E+08	2.376323E+08	8.508085E+08	4.876312E+08	1.578380E+09	4.317629E+08	8.891095E+08	1.942945E+09	1.894741E+08	**1.487113E+07**
CEC2017-F13	Avg	**1.113769E+05**	1.703238E+07	4.259176E+09	8.983917E+06	2.572675E+08	7.934088E+06	9.283913E+08	3.270202E+07	3.113209E+08	2.583705E+09	2.403875E+05	1.666033E+05
	Std	**5.854180E+04**	2.928689E+07	8.624498E+08	7.844219E+06	3.183773E+08	2.168756E+07	1.989082E+09	7.671117E+07	2.481980E+08	1.072966E+09	5.559129E+05	8.775156E+04
CEC2017-F14	Avg	**2.002495E+05**	2.361593E+05	2.181828E+06	2.657645E+06	1.435019E+06	6.315512E+05	8.236055E+05	6.972810E+05	2.243050E+05	5.840827E+06	7.324990E+05	4.893474E+05
	Std	**2.913784E+05**	3.454232E+05	6.512258E+05	2.662932E+06	8.130195E+05	7.288754E+05	8.037233E+05	6.799783E+05	3.962259E+05	2.768501E+06	7.125494E+05	9.072238E+05
CEC2017-F15	Avg	3.007711E+04	2.779665E+05	1.276156E+08	8.213319E+06	**1.501013E+04**	5.246670E+04	7.424881E+06	3.443943E+05	1.396133E+06	3.125704E+08	4.415064E+04	7.138984E+04
	Std	2.609275E+04	3.824570E+05	4.865416E+07	1.184999E+07	**3.066328E+03**	4.001566E+04	2.285287E+07	6.010366E+05	2.217606E+06	1.930435E+08	4.194547E+04	3.808096E+04
CEC2017-F16	Avg	2.896424E+03	2.957781E+03	4.651192E+03	4.317162E+03	4.171329E+03	3.143985E+03	3.327865E+03	3.553357E+03	3.764785E+03	5.156357E+03	3.394254E+03	**2.642188E+03**
	Std	3.603498E+02	3.898769E+02	2.971673E+02	7.375447E+02	4.471771E+02	3.491726E+02	4.082041E+02	5.066439E+02	3.622310E+02	3.937477E+02	4.755323E+02	**2.825674E+02**
CEC2017-F17	Avg	2.331028E+03	**2.192129E+03**	3.195927E+03	2.813578E+03	2.959737E+03	2.519953E+03	2.487510E+03	2.455521E+03	2.654718E+03	3.353859E+03	2.553037E+03	2.202601E+03

	Std	2.437904E+02	2.072216E+02	**1.942378E+02**	2.710238E+02	2.353446E+02	2.372963E+02	2.356910E+02	2.229336E+02	2.152313E+02	2.641161E+02	2.563435E+02	2.212974E+02
CEC2017-F18	Avg	**1.040106E+06**	3.023718E+06	1.286941E+07	1.419009E+07	4.421573E+06	7.475586E+06	7.749798E+06	2.836846E+06	2.890166E+06	5.495739E+07	1.239043E+06	1.922046E+06
	Std	**8.109684E+05**	2.866670E+06	4.979592E+06	1.596877E+07	4.275430E+06	1.095599E+07	9.017649E+06	2.690989E+06	3.455688E+06	3.556516E+07	1.041430E+06	2.684122E+06
CEC2017-F19	Avg	**5.249924E+04**	1.117129E+06	1.428533E+08	2.931891E+07	8.416937E+05	1.879073E+06	4.685757E+07	4.379348E+06	1.345015E+07	4.462067E+08	2.896388E+06	3.495290E+05
	Std	**6.022654E+04**	1.652488E+06	2.863104E+07	2.860517E+07	4.718328E+05	6.446304E+06	1.157002E+08	4.211076E+06	1.488191E+07	2.505900E+08	2.230248E+06	2.362524E+05
CEC2017-F20	Avg	2.585393E+03	2.604204E+03	2.893571E+03	2.986271E+03	3.094312E+03	2.749996E+03	2.842060E+03	2.748683E+03	2.894279E+03	3.325706E+03	2.574007E+03	**2.431787E+03**
	Std	1.826887E+02	1.825898E+02	**1.086060E+02**	2.022593E+02	2.542430E+02	2.156737E+02	2.259878E+02	1.794619E+02	1.940118E+02	1.819636E+02	1.264005E+02	1.825670E+02
CEC2017-F21	Avg	2.455595E+03	2.450829E+03	2.635238E+03	2.668566E+03	2.651419E+03	2.506880E+03	2.557243E+03	2.569084E+03	2.603613E+03	2.695909E+03	2.548607E+03	**2.393343E+03**
	Std	3.402081E+01	3.522961E+01	**1.617804E+01**	7.762668E+01	5.050096E+01	3.339159E+01	4.310358E+01	4.691987E+01	3.897070E+01	3.764364E+01	6.133248E+01	2.861099E+01
CEC2017-F22	Avg	5.159641E+03	7.206427E+03	6.056548E+03	8.533053E+03	7.570529E+03	6.625545E+03	7.420128E+03	**4.663328E+03**	6.163447E+03	8.204174E+03	5.331568E+03	4.868311E+03
	Std	2.108744E+03	1.443614E+03	**2.649012E+02**	1.256040E+03	4.890403E+02	1.105873E+03	1.848934E+03	1.716031E+03	2.489553E+03	1.557728E+03	2.030352E+03	1.723244E+03
CEC2017-F23	Avg	2.838297E+03	2.817967E+03	3.300235E+03	3.141750E+03	3.956994E+03	2.840998E+03	3.072238E+03	3.018176E+03	3.058453E+03	3.375844E+03	3.010039E+03	**2.784565E+03**
	Std	4.786253E+01	4.497355E+01	4.651251E+01	7.784277E+01	2.570963E+02	**4.202219E+01**	1.227855E+02	9.311407E+01	6.853995E+01	9.208826E+01	9.743730E+01	4.753237E+01
CEC2017-F24	Avg	2.976837E+03	2.977398E+03	3.544744E+03	3.283469E+03	3.955376E+03	2.979540E+03	3.283479E+03	3.162106E+03	3.217313E+03	3.559611E+03	3.219847E+03	**2.939539E+03**
	Std	6.182072E+01	4.085400E+01	4.897454E+01	9.045647E+01	1.527432E+02	**3.512252E+01**	6.336170E+01	7.849411E+01	7.602510E+01	1.037871E+02	7.954356E+01	3.644022E+01
CEC2017-F25	Avg	2.983517E+03	3.019958E+03	3.601527E+03	3.209281E+03	3.271976E+03	3.384390E+03	3.314866E+03	3.136792E+03	3.366829E+03	4.898569E+03	3.046768E+03	**2.965047E+03**
	Std	**3.247691E+01**	5.368088E+01	9.190737E+01	7.658864E+01	7.565097E+01	5.348935E+02	2.011735E+02	8.118905E+01	1.637567E+02	5.103242E+02	3.992148E+01	3.466955E+01
CEC2017-F26	Avg	5.833057E+03	5.399674E+03	8.888667E+03	8.753712E+03	9.052198E+03	5.821246E+03	7.394879E+03	7.193243E+03	7.212326E+03	9.920584E+03	7.393894E+03	**4.993820E+03**
	Std	1.064254E+03	4.250331E+02	**4.047694E+02**	1.278142E+03	5.273018E+02	4.505047E+02	9.793703E+02	1.380471E+03	1.276016E+03	6.056359E+02	1.645935E+03	1.122077E+03
CEC2017-F27	Avg	3.294889E+03	3.274819E+03	3.931984E+03	3.456583E+03	5.339480E+03	**3.257277E+03**	3.536737E+03	3.392281E+03	3.459256E+03	4.186126E+03	3.505406E+03	3.284546E+03
	Std	5.564487E+01	**2.854436E+01**	9.922771E+01	1.397315E+02	4.984728E+02	3.309649E+01	1.396532E+02	8.160896E+01	1.263406E+02	2.239813E+02	1.613445E+02	4.986707E+01
CEC2017-F28	Avg	3.491328E+03	3.445438E+03	5.147198E+03	3.994926E+03	4.494527E+03	4.432724E+03	4.134939E+03	3.792565E+03	4.087959E+03	6.169032E+03	3.492478E+03	**3.365645E+03**
	Std	2.090813E+02	1.322846E+02	1.133883E+02	3.218786E+02	2.298946E+02	8.281998E+02	3.848572E+02	2.697101E+02	3.221239E+02	5.553078E+02	9.437981E+01	**7.177440E+01**
CEC2017-F29	Avg	4.388238E+03	4.278080E+03	5.548386E+03	5.524068E+03	6.359164E+03	4.170358E+03	4.594398E+03	5.027340E+03	5.082877E+03	6.487003E+03	5.039855E+03	**4.136125E+03**
	Std	3.576903E+02	2.455966E+02	2.252158E+02	5.416960E+02	3.907198E+02	2.863959E+02	3.025105E+02	2.599515E+02	4.644431E+02	5.513472E+02	5.179266E+02	**2.043404E+02**
CEC2017-F30	Avg	3.144236E+06	5.956678E+06	7.348291E+08	7.795102E+07	2.134460E+07	**7.320515E+05**	1.218821E+07	4.138157E+07	9.899737E+07	4.669010E+08	2.582148E+07	1.860539E+06
	Std	3.248248E+06	5.085757E+06	1.806985E+08	6.564104E+07	2.553761E+07	**1.034619E+06**	9.173631E+06	4.086722E+07	6.226599E+07	2.115147E+08	3.089880E+07	1.196481E+06

Table 7 Comparison results on CEC2017 (Dim=50)

Algorithm	Metric	MELGWO	HSCA	GQPSO	WOA	GSA	MFO	SCHO	PO	NRBO	CPO	HO	DLBO

CEC2017-F1	Avg	1.401042E+10	1.163715E+10	6.601088E+10	2.019652E+10	5.898459E+10	2.942791E+10	3.553801E+10	3.773388E+10	5.584303E+10	9.412280E+10	1.041734E+10	**2.178307E+09**
	Std	5.645074E+09	4.935557E+09	2.118837E+09	4.461433E+09	7.787022E+09	1.849658E+10	8.695105E+09	9.906337E+09	6.220529E+09	1.048728E+10	2.754809E+09	**1.169026E+09**
CEC2017-F2	Avg	2.335206E+60	**8.429980E+54**	1.903431E+71	5.854879E+79	2.422824E+83	1.344725E+72	5.444800E+70	1.910304E+71	4.089575E+66	2.869436E+79	8.449455E+64	1.500028E+57
	Std	1.279045E+61	**3.494133E+55**	5.999214E+71	3.198460E+80	6.704339E+83	4.090152E+72	2.982240E+71	1.046305E+72	2.184271E+67	1.068984E+80	4.047508E+65	8.209721E+57
CEC2017-F3	Avg	1.357694E+05	3.108914E+05	1.634006E+05	3.188690E+05	2.019724E+05	4.297872E+05	2.683290E+05	1.423143E+05	1.592899E+05	4.148992E+05	**1.327771E+05**	2.576815E+05
	Std	2.753041E+04	9.238818E+04	1.279600E+04	1.043975E+05	2.257574E+04	8.669637E+04	6.755642E+04	1.585742E+04	3.532301E+04	1.665117E+05	**1.145540E+04**	8.434961E+04
CEC2017-F4	Avg	2.244927E+03	1.599636E+03	1.600038E+04	4.869621E+03	1.584393E+04	5.286209E+03	6.707933E+03	5.394672E+03	8.588714E+03	2.558432E+04	2.346267E+03	**1.017480E+03**
	Std	8.108745E+02	6.235922E+02	1.500120E+03	1.345806E+03	2.431007E+03	3.586305E+03	2.462661E+03	1.790116E+03	2.586245E+03	4.315714E+03	6.383543E+02	**1.848508E+02**
CEC2017-F5	Avg	8.387316E+02	8.908891E+02	1.116510E+03	1.097483E+03	8.458368E+02	1.007167E+03	1.023737E+03	1.026181E+03	1.108932E+03	1.248990E+03	8.890178E+02	**7.244549E+02**
	Std	4.398521E+01	6.486610E+01	**2.334541E+01**	7.610237E+01	3.036747E+01	7.944388E+01	4.766123E+01	4.216473E+01	3.999816E+01	3.424721E+01	3.551530E+01	5.233108E+01
CEC2017-F6	Avg	6.575447E+02	6.471550E+02	6.910522E+02	6.975798E+02	6.678664E+02	6.580318E+02	6.837414E+02	6.835185E+02	6.914936E+02	7.036292E+02	6.731750E+02	**6.361769E+02**
	Std	7.766347E+00	1.052529E+01	**3.163717E+00**	8.218747E+00	4.200918E+00	9.263327E+00	1.442682E+01	6.700637E+00	7.672805E+00	9.353521E+00	4.889864E+00	7.718957E+00
CEC2017-F7	Avg	1.417473E+03	1.358368E+03	1.756461E+03	1.911463E+03	1.612427E+03	2.187570E+03	1.662753E+03	1.822715E+03	1.815329E+03	2.167729E+03	1.688752E+03	**1.151403E+03**
	Std	1.124170E+02	8.329893E+01	**2.822970E+01**	8.884070E+01	1.142212E+02	3.998662E+02	7.798013E+01	9.821906E+01	9.765569E+01	1.189669E+02	6.654861E+01	1.218078E+02
CEC2017-F8	Avg	1.153151E+03	1.190383E+03	1.395298E+03	1.392369E+03	1.179836E+03	1.280099E+03	1.327428E+03	1.348578E+03	1.443581E+03	1.538897E+03	1.176588E+03	**1.036670E+03**
	Std	5.238564E+01	5.862598E+01	**2.155121E+01**	9.115275E+01	2.543985E+01	7.899369E+01	4.776851E+01	4.781996E+01	3.932851E+01	3.963370E+01	3.096939E+01	5.073465E+01
CEC2017-F9	Avg	1.292847E+04	2.053124E+04	3.175383E+04	3.964122E+04	1.321119E+04	1.878684E+04	4.396519E+04	2.668115E+04	2.919731E+04	4.599823E+04	2.028898E+04	**5.987664E+03**
	Std	2.322043E+03	9.504804E+03	2.254655E+03	9.704231E+03	**1.045673E+03**	4.785666E+03	8.215693E+03	3.682767E+03	3.161227E+03	5.683910E+03	2.663976E+03	1.862233E+03
CEC2017-F10	Avg	8.490410E+03	1.100178E+04	1.495391E+04	1.356855E+04	8.877586E+03	8.832364E+03	1.211986E+04	1.174868E+04	1.412641E+04	1.651622E+04	9.572593E+03	**7.619196E+03**
	Std	9.154805E+02	1.377661E+03	**4.903654E+02**	1.025458E+03	8.229531E+02	1.116996E+03	1.052967E+03	8.240761E+02	7.236319E+02	4.933821E+02	1.059060E+03	1.012174E+03
CEC2017-F11	Avg	4.483179E+03	**3.322025E+03**	1.464295E+04	9.024402E+03	2.658637E+04	1.695194E+04	1.104516E+04	6.244476E+03	1.043344E+04	2.987759E+04	4.989456E+03	3.696341E+03
	Std	2.241984E+03	**7.673479E+02**	1.253139E+03	1.819662E+03	3.778554E+03	9.423721E+03	4.066557E+03	2.162958E+03	2.529488E+03	6.477605E+03	1.336029E+03	2.288160E+03
CEC2017-F12	Avg	2.004898E+09	9.781238E+08	4.222246E+10	4.508790E+09	3.866275E+10	5.931995E+09	1.088582E+10	7.632831E+09	1.626272E+10	4.814647E+10	1.290727E+09	**1.940455E+08**
	Std	2.007435E+09	7.158717E+08	3.287390E+09	1.691429E+09	7.102777E+09	4.504133E+09	7.813437E+09	4.377948E+09	5.637163E+09	1.063893E+10	5.059570E+08	**2.034949E+08**
CEC2017-F13	Avg	3.002621E+08	1.732204E+08	1.954607E+10	5.689785E+08	1.823881E+10	8.156931E+08	5.524034E+09	4.190897E+08	4.319589E+09	1.867472E+10	4.016164E+06	**3.144024E+05**
	Std	1.369911E+09	1.861722E+08	2.901773E+09	3.611329E+08	6.323510E+09	1.145640E+09	6.386510E+09	6.488366E+08	2.236838E+09	5.289667E+09	1.185794E+07	**1.646886E+05**
CEC2017-F14	Avg	**1.050401E+06**	1.870336E+06	2.374472E+07	7.855762E+06	4.217974E+07	2.503384E+06	8.584534E+06	2.695184E+06	3.540391E+06	4.615340E+07	2.729352E+06	1.769255E+06
	Std	**1.271816E+06**	2.257054E+06	8.231613E+06	6.037198E+06	2.384554E+07	5.379069E+06	1.563308E+07	2.886425E+06	4.448616E+06	2.671894E+07	2.495638E+06	2.115758E+06
CEC2017-F15	Avg	4.150570E+06	1.717328E+07	2.938126E+09	8.828980E+07	8.182938E+08	9.329889E+07	3.755727E+08	9.799322E+07	3.787459E+08	3.595698E+09	6.184326E+05	**9.657109E+04**
	Std	1.338499E+07	3.106085E+07	4.287702E+08	1.356259E+08	7.381311E+08	2.458627E+08	5.863901E+08	1.694677E+08	2.366875E+08	1.827155E+09	1.930143E+06	**3.490256E+04**
CEC2017-F16	Avg	3.906850E+03	4.144625E+03	6.626125E+03	6.446299E+03	6.326184E+03	4.377303E+03	4.730739E+03	5.134982E+03	5.867092E+03	7.912844E+03	5.324498E+03	**3.713904E+03**

	Std	5.188556E+02	6.443282E+02	**2.674177E+02**	9.774592E+02	7.108230E+02	6.674748E+02	6.728485E+02	8.176726E+02	7.433487E+02	6.519595E+02	7.411536E+02	4.040661E+02
CEC2017-F17	Avg	3.586904E+03	3.482148E+03	5.589442E+03	4.781930E+03	4.250628E+03	4.132815E+03	4.003556E+03	4.360023E+03	4.478203E+03	6.653071E+03	3.832055E+03	**3.336779E+03**
	Std	3.865004E+02	3.651269E+02	3.413178E+02	6.072824E+02	4.344652E+02	5.304354E+02	5.311783E+02	5.037629E+02	4.088992E+02	1.544611E+03	4.175933E+02	**3.203480E+02**
CEC2017-F18	Avg	6.649930E+06	8.871135E+06	7.780603E+07	6.353213E+07	4.122657E+07	1.679153E+07	1.915512E+07	2.462981E+07	2.145958E+07	1.721545E+08	7.005875E+06	**4.121586E+06**
	Std	7.423822E+06	7.061115E+06	2.242506E+07	4.232405E+07	1.406571E+07	2.962384E+07	2.119758E+07	2.109784E+07	1.904634E+07	6.892303E+07	6.462647E+06	**3.735783E+06**
CEC2017-F19	Avg	**1.060013E+06**	7.132732E+06	1.457468E+09	2.062955E+07	6.676871E+07	1.055048E+08	3.454000E+08	7.930569E+07	2.046354E+08	1.374816E+09	9.827490E+06	1.197723E+06
	Std	2.807492E+06	9.021768E+06	3.311662E+08	1.733272E+07	1.420378E+08	3.601028E+08	8.207737E+08	1.554887E+08	1.247025E+08	5.443396E+08	9.827439E+06	**5.229144E+05**
CEC2017-F20	Avg	3.278102E+03	3.494208E+03	4.046505E+03	4.074328E+03	3.883195E+03	3.700326E+03	3.764484E+03	3.700950E+03	3.881436E+03	4.886342E+03	3.277446E+03	**3.138090E+03**
	Std	3.140977E+02	3.668785E+02	**1.454306E+02**	3.660292E+02	3.464483E+02	3.993840E+02	3.538767E+02	2.911680E+02	2.672567E+02	2.272283E+02	2.123542E+02	2.461945E+02
CEC2017-F21	Avg	2.641468E+03	2.664716E+03	2.977709E+03	3.087118E+03	2.967743E+03	2.756235E+03	2.872031E+03	2.842331E+03	2.960286E+03	3.091830E+03	2.806929E+03	**2.517971E+03**
	Std	4.405644E+01	6.942971E+01	**2.188569E+01**	1.076857E+02	6.176680E+01	8.474255E+01	7.753006E+01	6.553960E+01	6.392143E+01	4.214751E+01	7.853988E+01	5.371895E+01
CEC2017-F22	Avg	1.038183E+04	1.248595E+04	1.664537E+04	1.484303E+04	1.210372E+04	1.055952E+04	1.461963E+04	1.434491E+04	1.581472E+04	1.820500E+04	1.167533E+04	**8.902348E+03**
	Std	9.756460E+02	1.085123E+03	6.280169E+02	1.155754E+03	8.556004E+02	9.002955E+02	1.009398E+03	9.714710E+02	8.704715E+02	**4.787029E+02**	1.113716E+03	1.945595E+03
CEC2017-F23	Avg	3.200700E+03	3.159534E+03	3.951420E+03	3.895875E+03	5.098195E+03	3.187209E+03	3.663293E+03	3.572642E+03	3.653612E+03	4.165100E+03	3.575506E+03	**3.068072E+03**
	Std	8.410991E+01	6.313475E+01	**6.140788E+01**	1.597421E+02	2.693829E+02	7.833632E+01	1.390715E+02	1.261244E+02	1.253573E+02	1.817435E+02	1.630678E+02	8.356476E+01
CEC2017-F24	Avg	3.300031E+03	3.296072E+03	4.567504E+03	3.932284E+03	5.349586E+03	3.247900E+03	3.869180E+03	3.720766E+03	3.798389E+03	4.569826E+03	3.954511E+03	**3.242663E+03**
	Std	8.734772E+01	6.735481E+01	7.528525E+01	1.704017E+02	1.950495E+02	**6.361280E+01**	1.700581E+02	1.547057E+02	1.120060E+02	2.325199E+02	2.212944E+02	1.044040E+02
CEC2017-F25	Avg	4.087099E+03	3.942371E+03	8.320110E+03	5.202417E+03	8.883222E+03	5.578298E+03	5.769051E+03	5.788314E+03	7.162246E+03	1.439882E+04	4.241448E+03	**3.673784E+03**
	Std	3.545202E+02	3.249580E+02	**2.709297E+02**	4.547810E+02	7.810856E+02	1.924590E+03	9.677797E+02	9.638649E+02	9.409851E+02	1.526457E+03	3.700182E+02	3.180690E+02
CEC2017-F26	Avg	1.032071E+04	**7.966783E+03**	1.399619E+04	1.471383E+04	1.398056E+04	8.831038E+03	1.200569E+04	1.311551E+04	1.281626E+04	1.721377E+04	1.249600E+04	8.412102E+03
	Std	1.100983E+03	6.195452E+02	**3.433605E+02**	1.493941E+03	8.170550E+02	8.743547E+02	9.136440E+02	1.071174E+03	1.445047E+03	8.447844E+02	1.101583E+03	1.870513E+03
CEC2017-F27	Avg	3.851461E+03	3.859365E+03	6.314928E+03	4.822898E+03	9.010900E+03	**3.639805E+03**	4.749873E+03	4.150019E+03	4.465746E+03	6.567309E+03	4.487162E+03	3.777390E+03
	Std	1.880585E+02	1.404354E+02	2.234433E+02	5.126930E+02	7.772598E+02	**1.353742E+02**	3.205429E+02	2.221074E+02	3.137389E+02	3.778846E+02	3.219506E+02	1.892607E+02
CEC2017-F28	Avg	4.961670E+03	4.950122E+03	8.184740E+03	6.238340E+03	9.110145E+03	8.175883E+03	6.354628E+03	6.159567E+03	7.285818E+03	1.125108E+04	4.966138E+03	**4.525917E+03**
	Std	4.055626E+02	6.175460E+02	**1.666178E+02**	4.808489E+02	5.594189E+02	1.488288E+03	6.841152E+02	5.907658E+02	6.647184E+02	7.992375E+02	3.890650E+02	5.686414E+02
CEC2017-F29	Avg	5.974159E+03	5.556520E+03	1.476246E+04	9.299211E+03	2.921981E+04	**5.263227E+03**	6.996368E+03	7.908407E+03	8.330353E+03	1.768465E+04	8.316796E+03	5.318443E+03
	Std	6.877733E+02	**5.482772E+02**	1.851327E+03	1.697864E+03	1.163225E+04	5.595118E+02	9.559698E+02	8.386642E+02	1.163377E+03	6.026150E+03	1.286293E+03	5.916225E+02
CEC2017-F30	Avg	1.015146E+08	1.472617E+08	2.456624E+09	3.670825E+08	1.120003E+09	**4.397188E+07**	7.769991E+08	3.040483E+08	7.118034E+08	3.501030E+09	2.733166E+08	5.426944E+07
	Std	4.989044E+07	5.402433E+07	4.574947E+08	1.599862E+08	6.515704E+08	8.214164E+07	1.077874E+09	1.637174E+08	2.708518E+08	9.912619E+08	1.048276E+08	**1.761620E+07**

Table 8 Comparison results on CEC2017 (Dim=100)

Algorithm	Metric	MELGWO	HSCA	GQPSO	WOA	GSA	MFO	SCHO	PO	NRBO	CPO	HO	DLBO
CEC2017-F1	Avg	7.506969E+10	6.468127E+10	1.906267E+11	1.099481E+11	2.142553E+11	1.407718E+11	1.209636E+11	1.375625E+11	1.690778E+11	2.596770E+11	7.404729E+10	**5.049510E+10**
	Std	1.944927E+10	1.472295E+10	**5.035987E+09**	1.071333E+10	1.613359E+10	4.093328E+10	1.546293E+10	1.443507E+10	1.324739E+10	1.841860E+10	9.197225E+09	1.150539E+10
CEC2017-F2	Avg	**2.349909E+141**	1.645990E+147	4.916213E+157	4.763361E+170	3.786263E+183	2.913749E+171	1.683128E+155	1.896959E+154	2.976555E+155	7.077144E+170	9.454960E+159	3.853339E+141
	Std	8.859022E+141	9.015456E+147	**6.553500E+04**	**6.553500E+04**	**6.553500E+04**	**6.553500E+04**	**6.553500E+04**	**6.553500E+04**	**6.553500E+04**	**6.553500E+04**	**6.553500E+04**	2.082753E+142
CEC2017-F3	Avg	5.920118E+05	9.818754E+05	3.508782E+05	9.300490E+05	3.776111E+05	1.006292E+06	4.624165E+05	**3.198357E+05**	3.784956E+05	8.723751E+06	3.201926E+05	6.354944E+05
	Std	1.251441E+05	1.321301E+05	1.798292E+04	1.214607E+05	2.109395E+04	1.977355E+05	1.110836E+05	1.473504E+04	6.072026E+04	2.042834E+07	**1.020871E+04**	1.168949E+05
CEC2017-F4	Avg	1.081851E+04	6.831412E+03	5.089763E+04	2.261493E+04	6.742265E+04	3.303388E+04	2.004682E+04	2.022627E+04	2.886365E+04	8.475573E+04	1.202857E+04	**5.883985E+03**
	Std	4.042108E+03	**1.661308E+03**	4.033493E+03	4.680206E+03	8.955238E+03	1.462679E+04	5.662293E+03	4.865425E+03	5.442259E+03	1.166730E+04	2.180804E+03	2.105957E+03
CEC2017-F5	Avg	1.440116E+03	1.579458E+03	1.974234E+03	1.911755E+03	1.557060E+03	1.980222E+03	1.854163E+03	1.815256E+03	2.012710E+03	2.226937E+03	1.511482E+03	**1.239537E+03**
	Std	7.273683E+01	1.204002E+02	**1.913110E+01**	7.689872E+01	7.499120E+01	1.659617E+02	8.896821E+01	6.447858E+01	5.632963E+01	5.915870E+01	4.550882E+01	9.998591E+01
CEC2017-F6	Avg	6.721896E+02	6.760942E+02	7.053474E+02	7.057946E+02	6.749184E+02	6.844609E+02	6.978049E+02	6.962957E+02	7.033668E+02	7.176401E+02	6.835675E+02	**6.565623E+02**
	Std	4.870188E+00	1.356788E+01	**2.112611E+00**	6.939910E+00	3.090248E+00	7.526616E+00	7.138940E+00	4.481107E+00	5.175449E+00	5.281643E+00	3.336338E+00	5.270615E+00
CEC2017-F7	Avg	3.022122E+03	2.872273E+03	3.535365E+03	3.802512E+03	3.359413E+03	5.621000E+03	3.351328E+03	3.671874E+03	3.707880E+03	4.214193E+03	3.410418E+03	**2.705531E+03**
	Std	1.323802E+02	1.589745E+02	**8.402813E+01**	2.112368E+02	1.535675E+02	6.752075E+02	1.955019E+02	1.057968E+02	1.958634E+02	1.311656E+02	1.169409E+02	4.061815E+02
CEC2017-F8	Avg	1.850917E+03	1.897220E+03	2.347613E+03	2.396767E+03	1.999527E+03	2.278254E+03	2.187789E+03	2.317875E+03	2.439140E+03	2.642914E+03	1.991694E+03	**1.579960E+03**
	Std	8.689559E+01	1.140674E+02	**3.678142E+01**	1.171820E+02	8.155289E+01	1.457021E+02	1.053562E+02	6.298284E+01	9.068506E+01	6.497965E+01	7.142637E+01	1.295963E+02
CEC2017-F9	Avg	3.313800E+04	6.966293E+04	7.073545E+04	8.152376E+04	3.110614E+04	5.900286E+04	9.831908E+04	6.052928E+04	7.186228E+04	1.075690E+05	4.671629E+04	**2.742819E+04**
	Std	6.273915E+03	1.613331E+04	3.951139E+03	2.201215E+04	**2.449860E+03**	8.653623E+03	3.747335E+03	5.415623E+03	5.121650E+03	1.100466E+04	5.302595E+03	1.132666E+04
CEC2017-F10	Avg	1.986441E+04	2.504904E+04	3.221669E+04	2.949462E+04	2.107128E+04	1.972159E+04	2.839333E+04	2.771278E+04	3.070186E+04	3.444841E+04	2.071434E+04	**1.607499E+04**
	Std	2.120369E+03	2.285984E+03	6.571582E+02	1.595455E+03	1.592648E+03	1.451036E+03	1.598205E+03	1.765684E+03	1.337017E+03	**6.248206E+02**	1.828954E+03	1.204750E+03
CEC2017-F11	Avg	**6.575608E+04**	1.082485E+05	1.642291E+05	2.978086E+05	1.946274E+05	2.183111E+05	1.261138E+05	1.104633E+05	1.171272E+05	4.013100E+05	1.188877E+05	1.551289E+05
	Std	**1.384117E+04**	3.591044E+04	1.631475E+04	1.165337E+05	2.121376E+04	7.604884E+04	2.975417E+04	1.997787E+04	1.858802E+04	9.804472E+04	1.792723E+04	6.135191E+04
CEC2017-F12	Avg	2.240818E+10	1.065262E+10	1.219811E+11	3.158227E+10	1.510762E+11	3.901044E+10	5.498400E+10	4.262456E+10	6.922272E+10	1.463506E+11	1.566755E+10	**2.822288E+09**
	Std	8.321044E+09	3.864004E+09	5.892625E+09	6.250963E+09	1.778475E+10	2.087348E+10	1.488840E+10	1.375460E+10	1.441964E+10	1.894182E+10	3.684439E+09	**1.406768E+09**
CEC2017-F13	Avg	2.656240E+09	1.186593E+09	2.746095E+10	3.079101E+09	3.111830E+10	4.331507E+09	1.076101E+10	6.858006E+09	1.434803E+10	3.227615E+10	5.260659E+08	**8.928546E+05**
	Std	2.206184E+09	1.056212E+09	1.739874E+09	1.983574E+09	4.671379E+09	4.551139E+09	5.217130E+09	3.543769E+09	4.244165E+09	6.095875E+09	3.827034E+08	**3.057470E+06**
CEC2017-F14	Avg	**5.426123E+06**	1.168843E+07	3.035525E+07	2.145577E+07	3.152747E+07	2.342002E+07	1.762330E+07	1.493515E+07	2.681155E+07	1.186604E+08	8.676050E+06	1.006715E+07
	Std	4.010014E+06	6.365072E+06	4.860644E+06	9.357112E+06	2.018041E+07	2.176902E+07	7.380862E+06	7.280835E+06	9.904015E+06	3.641436E+07	**3.324123E+06**	6.366737E+06
CEC2017-F15	Avg	3.782298E+08	1.749650E+08	1.236179E+10	4.537023E+08	1.429391E+10	1.411032E+09	3.327759E+09	1.723091E+09	5.052322E+09	1.363429E+10	8.985049E+05	**4.015227E+05**
	Std	9.658331E+08	1.762335E+08	1.248885E+09	2.680176E+08	2.258703E+09	1.334692E+09	2.343403E+09	1.333049E+09	2.189685E+09	3.473002E+09	2.262957E+06	**1.266997E+06**

CEC2017-F16	Avg	8.217239E+03	8.515477E+03	1.685412E+04	1.685224E+04	1.786543E+04	8.597513E+03	1.153677E+04	1.367114E+04	1.465980E+04	1.905111E+04	1.123533E+04	**7.016660E+03**
	Std	9.927499E+02	8.146954E+02	**6.617973E+02**	2.083717E+03	1.255476E+03	1.226901E+03	1.529758E+03	2.000721E+03	1.244812E+03	1.720086E+03	1.555238E+03	6.957396E+02
CEC2017-F17	Avg	8.630449E+03	6.245588E+03	2.549031E+05	2.750497E+04	5.449368E+06	1.108294E+04	5.337683E+04	3.342451E+04	8.333664E+04	1.427920E+06	8.275466E+03	**5.937841E+03**
	Std	6.924732E+03	**5.249695E+02**	8.002817E+04	2.145134E+04	2.990172E+06	9.565333E+03	8.099423E+04	4.145598E+04	7.825462E+04	1.353608E+06	1.138902E+03	6.728876E+02
CEC2017-F18	Avg	7.140001E+06	1.393583E+07	4.921380E+07	1.954600E+07	3.958191E+07	3.815363E+07	2.406162E+07	1.867346E+07	3.368147E+07	2.184301E+08	**6.290189E+06**	9.840263E+06
	Std	4.215752E+06	8.504718E+06	1.467667E+07	9.557228E+06	1.960289E+07	5.211465E+07	1.113648E+07	9.033967E+06	1.907782E+07	7.816943E+07	**3.275972E+06**	6.532848E+06
CEC2017-F19	Avg	1.834029E+08	1.840262E+08	1.134090E+10	6.202793E+08	1.412888E+10	8.509950E+08	2.803125E+09	1.663776E+09	3.528210E+09	1.362330E+10	3.984170E+07	**9.870338E+06**
	Std	4.146606E+08	1.915771E+08	1.099807E+09	4.154962E+08	2.789328E+09	1.225177E+09	2.524037E+09	1.313990E+09	1.151291E+09	2.997688E+09	3.653475E+07	**4.393156E+06**
CEC2017-F20	Avg	5.541673E+03	6.149456E+03	7.574771E+03	7.362757E+03	6.590702E+03	5.818613E+03	6.772515E+03	6.532936E+03	7.311184E+03	8.883502E+03	5.634570E+03	**4.877074E+03**
	Std	6.978779E+02	5.509752E+02	**3.076595E+02**	4.819837E+02	5.651223E+02	6.239762E+02	5.781267E+02	6.902661E+02	4.323173E+02	3.383600E+02	4.766920E+02	5.641047E+02
CEC2017-F21	Avg	3.406645E+03	3.458798E+03	4.123236E+03	4.440713E+03	5.398453E+03	3.801871E+03	4.042644E+03	4.041830E+03	4.122354E+03	4.554443E+03	3.908806E+03	**3.098444E+03**
	Std	1.238157E+02	1.327169E+02	**5.492079E+01**	2.329930E+02	2.861070E+02	1.756607E+02	1.171124E+02	1.851408E+02	1.592438E+02	1.318915E+02	1.601909E+02	1.193091E+02
CEC2017-F22	Avg	2.296594E+04	2.748213E+04	3.437516E+04	3.178126E+04	2.542866E+04	2.171463E+04	3.243168E+04	3.028037E+04	3.373570E+04	3.706662E+04	2.455661E+04	**1.927548E+04**
	Std	2.326124E+03	1.358237E+03	**6.395404E+02**	1.742760E+03	1.326052E+03	1.223721E+03	1.643245E+03	1.372522E+03	1.240438E+03	7.855841E+02	1.612241E+03	1.469374E+03
CEC2017-F23	Avg	4.004667E+03	4.072155E+03	6.768937E+03	5.350165E+03	8.495318E+03	**3.882077E+03**	5.363117E+03	4.933554E+03	5.049343E+03	6.701959E+03	5.077492E+03	3.947594E+03
	Std	1.437313E+02	1.492442E+02	2.056875E+02	2.596386E+02	6.719081E+02	**1.116311E+02**	3.477662E+02	2.092468E+02	2.372753E+02	3.694254E+02	3.505521E+02	3.125811E+02
CEC2017-F24	Avg	4.758661E+03	4.828884E+03	9.555452E+03	6.871178E+03	1.339464E+04	**4.529504E+03**	6.886769E+03	6.170804E+03	6.333135E+03	1.042635E+04	6.878749E+03	4.875884E+03
	Std	1.741405E+02	**1.634981E+02**	2.641167E+02	3.412726E+02	7.026352E+02	1.721578E+02	3.986670E+02	4.346131E+02	3.374192E+02	7.127507E+02	5.646637E+02	3.934404E+02
CEC2017-F25	Avg	8.393685E+03	8.345889E+03	1.747236E+04	1.096178E+04	2.064610E+04	1.954203E+04	1.193170E+04	1.345217E+04	1.550052E+04	2.907044E+04	7.900972E+03	**7.306492E+03**
	Std	1.152586E+03	1.192130E+03	**3.501790E+02**	9.122761E+02	2.126321E+03	6.660730E+03	2.071929E+03	1.523592E+03	1.323519E+03	2.714576E+03	6.073468E+02	1.305144E+03
CEC2017-F26	Avg	2.496306E+04	**1.947172E+04**	3.748018E+04	3.790238E+04	4.675823E+04	1.961777E+04	3.213692E+04	3.718668E+04	3.725441E+04	5.030903E+04	3.251073E+04	2.265906E+04
	Std	4.656912E+03	1.223946E+03	**6.427339E+02**	3.740775E+03	2.624236E+03	1.572969E+03	2.182267E+03	2.447424E+03	3.283855E+03	3.914378E+03	2.571756E+03	3.805268E+03
CEC2017-F27	Avg	4.621007E+03	4.675904E+03	1.075375E+04	6.235084E+03	1.694576E+04	**4.038176E+03**	6.918742E+03	5.285816E+03	6.325032E+03	1.187129E+04	5.893553E+03	4.410110E+03
	Std	3.224508E+02	3.240471E+02	6.070292E+02	9.181095E+02	1.012374E+03	**1.949837E+02**	7.885985E+02	6.499485E+02	5.790430E+02	9.706564E+02	7.032937E+02	2.627855E+02
CEC2017-F28	Avg	**1.004899E+04**	1.138775E+04	1.917437E+04	1.526676E+04	2.756788E+04	2.036960E+04	1.572140E+04	1.514203E+04	2.061193E+04	3.203605E+04	1.108982E+04	1.085549E+04
	Std	1.393238E+03	1.516765E+03	**4.916078E+02**	1.003415E+03	2.088457E+03	2.395197E+03	2.256931E+03	1.172511E+03	1.593853E+03	2.662413E+03	9.800687E+02	1.943926E+03
CEC2017-F29	Avg	1.249945E+04	**1.017792E+04**	7.853815E+04	2.082392E+04	2.558318E+05	1.207269E+04	2.399106E+04	2.350771E+04	2.460270E+04	2.128894E+05	1.663552E+04	1.062721E+04
	Std	2.339870E+03	**1.170776E+03**	2.176055E+04	4.222118E+03	1.627289E+05	5.006318E+03	1.793298E+04	8.687959E+03	5.756571E+03	1.577745E+05	1.734922E+03	1.198860E+03
CEC2017-F30	Avg	2.204059E+09	9.715315E+08	2.649168E+10	3.115361E+09	2.950278E+10	3.160881E+09	8.752717E+09	6.224000E+09	1.248088E+10	2.704783E+10	1.260872E+09	**1.726093E+08**
	Std	1.785461E+09	6.242139E+08	2.059364E+09	1.542578E+09	4.482937E+09	2.170470E+09	4.072556E+09	2.990364E+09	3.859491E+09	5.682434E+09	6.218841E+08	**9.543818E+07**

3.5 Statistical Analysis

This section uses rank tests and the Friedman test to verify the performance differences between DLBO and 11 other competing algorithms. These non-parametric statistical tests provide an objective comparison of the algorithms' performance across multiple experimental results, ensuring statistical significance and reliability of the analysis. This not only helps to demonstrate the superiority of DLBO but also provides strong statistical support for its application in various environments, thereby proving its overall competitiveness and practicality.

3.5.1 Wilcoxon signed-rank test

In this section, we apply the Wilcoxon signed-rank test to review the performance of DLBO together with the other competing algorithms, and the results are presented in **Table 8**. When the p-value is less than 0.05, the algorithm is considered to have a significant difference from DLBO. Conversely, when the p-value is more than 0.05, there is no significant difference between the two algorithms. The symbols '+/=/−' are used to indicate whether DLBO performs better than, similar to, or worse than the competitors. We can see clearly from the table that DLBO distinguishes from other competitors. Also, DLBO is insensitive to dimensional increase, consistently outperforming the remaining competitors.

From **Table 9**, we can see that DLBO outperforms the competitor in approximately 85% of the cases within both CEC2017 and CEC2022. Within CEC2017, DLBO is superior to the competitors in at least 20 functions, on average 26 functions. Within CEC2022, DLBO is superior to the competitors in at least 4 functions, on average 10 functions. The experimental outcomes further demonstrate the excellence of the purposed DLBO.

Table 9 Wilcoxon signed-rank test statistical results

DLBO vs.	CEC2017 (Dim=30)	CEC2017 (Dim=50)	CEC2017 (Dim=100)	CEC2022 (Dim=10)	CEC2022 (Dim=20)
MELGWO	20/6/4	21/7/2	23/5/2	4/3/5	8/2/2
HSCA	23/6/1	24/6/0	23/5/2	6/5/1	9/2/1
GQPSO	29/0/1	29/0/1	28/1/1	11/1/0	11/1/0
WOA	30/0/0	30/0/0	30/0/0	12/0/0	12/0/0
GSA	28/1/1	28/1/1	29/0/1	9/2/1	11/0/1
MFO	23/4/3	23/5/2	25/2/3	6/4/2	9/2/1
SCHO	29/1/0	29/1/0	28/1/1	12/0/0	11/1/0
PO	28/1/1	29/0/1	28/0/2	8/4/0	10/0/2
NRBO	26/3/1	29/0/1	28/0/2	10/2/0	11/0/1
CPO	30/0/0	30/0/0	30/0/0	11/1/0	12/0/0

HO	25/3/2	27/2/1	25/2/3	9/2/1	10/1/1
Overall	**291/25/14**	**299/22/9**	**297/16/17**	**98/24/10**	**114/9/9**

3.5.2 Friedman mean rank test

In this section, we apply the nonparametric Friedman mean rank test to evaluate and rank the DLBO performance among all the candidates on the test suites. The analysis results are included in **Table 10**. It is clear that DLBO consistently outperforms the other competitors. With CEC2017 at Dimension 30, DLBO achieves an average rank of 1.83. With CEC2017 at Dimension 50, DLBO achieves an average rank of 1.50. With CEC2017 at Dimension 100, DLBO achieves an average rank of 1.83. With CEC2022 at Dimension 10, DLBO achieves an average rank of 2.50. With CEC2022 at Dimension 20, DLBO achieves an average rank of 1.92. Across the two test sets within all dimensions, DLBO all achieves the top place in the result ranking, another strong evidence of the superiority of DLBO.

Table 10 Friedman mean rank test results.

Suites	**CEC2017**						**CEC2022**			
Dimensions	**30**		**50**		**100**		**10**		**20**	
Algorithms	Ave Rank	Overall Rank	Ave Rank	Overall Rank	Ave Rank	Overall Rank	Ave Rank	Overall Rank	Ave Rank	Overall Rank
MELGWO	2.47	2	2.67	2	2.90	2	2.58	2	2.83	2
HSCA	3.47	3	3.40	3	3.57	3	3.33	3	3.25	3
GQPSO	10.10	11	10.17	11	9.43	11	10.17	11	9.42	11
WOA	9.10	10	8.47	9	7.87	8	9.42	10	8.67	9
GSA	8.23	9	8.50	10	9.23	10	8.08	8	8.67	9
MFO	5.03	5	5.03	5	5.77	5	4.00	4	4.83	4
SCHO	7.30	7	7.07	7	7.10	7	8.75	9	8.00	7
PO	6.07	6	6.50	6	6.23	6	5.42	6	5.50	6
NRBO	7.77	8	8.30	8	8.50	9	7.25	7	8.33	8
CPO	11.67	12	11.73	12	11.57	12	11.25	12	11.33	12
HO	4.97	4	4.67	4	4.00	4	5.25	5	5.25	5
DLBO	**1.83**	**1**	**1.50**	**1**	**1.83**	**1**	**2.50**	**1**	**1.92**	**1**

4.Engineering design problems

This section presents four engineering design problems that demonstrate the superior efficiency and real-world applicability of DLBO

4.1 Tension/compression spring design

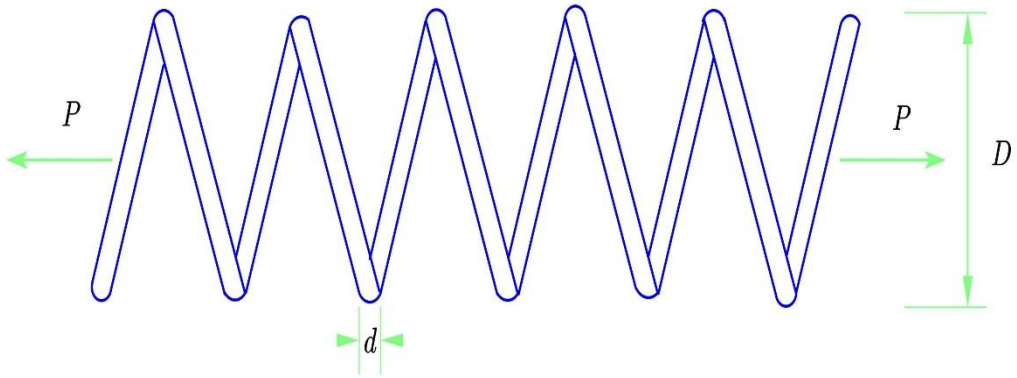

Fig.12. Tension/compression spring.

This problem is to minimize the weight $f(x)$ of a tension/compression spring subjected to four constraints. Three variables are used to depict this weight (as shown in **Fig. 12**): d (wire diameter, x_1), D (mean coil diameter, x_2), and P (the number of active coils, x_3). This problem can be formulated as follows:

Minimize:

$$f(x) = (x_3 + 2)x_2x_1^2 \tag{10}$$

Subject to:

$$g_1(x) = 1 - \frac{x_2^3 x_3}{717854x_1^4} \leq 0 \tag{11}$$

$$g_2(x) = 1 - \frac{4x_2^2 - x_1x_2}{12566(x_2x_1^3 - x_1^4)} + \frac{1}{5180x_1^2} - 1 \leq 0 \tag{12}$$

$$g_3(x) = 1 - \frac{140.45x_1}{x_2^2x_3} \leq 0 \tag{13}$$

$$g_4(x) = \frac{x_1 + x_2}{1.5} - 1 \leq 0 \tag{14}$$

Bound:

$$0.05 \leq x_1 \leq 2.00, 0.25, \leq x_2 \leq 1.30, 2.00 \leq x_3 \leq 15.00 \tag{15}$$

Table 11 Results of the Tension/compression spring problem.

Algorithm	x1	x2	x3	F(min)
MELGWO	5.80E-02	5.29E-01	5.49E+00	1.33E-02
HSCA	5.94E-02	5.71E-01	4.80E+00	1.37E-02
GQPSO	5.00E-02	3.15E-01	1.50E+01	1.34E-02
WOA	5.79E-02	5.24E-01	5.58E+00	1.33E-02
GSA	2.95E-01	6.09E-01	6.87E+00	5.44E+15
MFO	5.99E-02	5.87E-01	4.55E+00	1.38E-02
SCHO	6.23E-02	6.69E-01	3.63E+00	1.46E-02
PO	5.62E-02	4.75E-01	6.68E+00	1.30E-02
NRBO	5.00E-02	3.11E-01	1.50E+01	1.32E-02
CPO	6.45E-02	5.16E-01	9.15E+00	2.39E-02
HO	5.77E-02	5.19E-01	5.70E+00	1.33E-02
DLBO	**5.00E-02**	**3.16E-01**	**1.43E+01**	**1.29E-02**

Based on **Table 11** data analysis, the DLBO algorithm performed excellently in the tension/compression spring design problem, with the minimum objective function value $F_{min} = 1.29 \times 10^{-2}$ This is superior to other traditional algorithms such as MELGWO, HSCA, and GQPSO, demonstrating outstanding optimization capability and robustness. The optimization variable values for the DLBO algorithm are $x_1 = 5.00 \times 10^{-2}$, $x_2 = 3.16 \times 10^{-1}$, and $x_3 = 1.43 \times 10$, indicating that it found better parameter combinations for solving this engineering problem. These parameter combinations minimized the weight of the spring while satisfying the design constraints, validating the effectiveness of the DLBO algorithm in handling complex constrained optimization problems.

Further comparison reveals that DLBO effectively avoided local optima in high-dimensional and multimodal optimization problems, successfully finding the global optimal solution. For instance, the GSA algorithm performed poorly in high-dimensional situations, with its objective function value reaching 5.44×10^{15}, far higher than other algorithms, while DLBO maintained a consistently low objective function value. This indicates that the DLBO algorithm achieved a good balance between global and local search, exhibiting stronger adaptability and robustness, proving its wide applicability and superiority in engineering problems. Future work can further optimize the structure of the DLBO algorithm to enhance its performance in real-time or fast-response scenarios.

4.2 Pressure vessel design

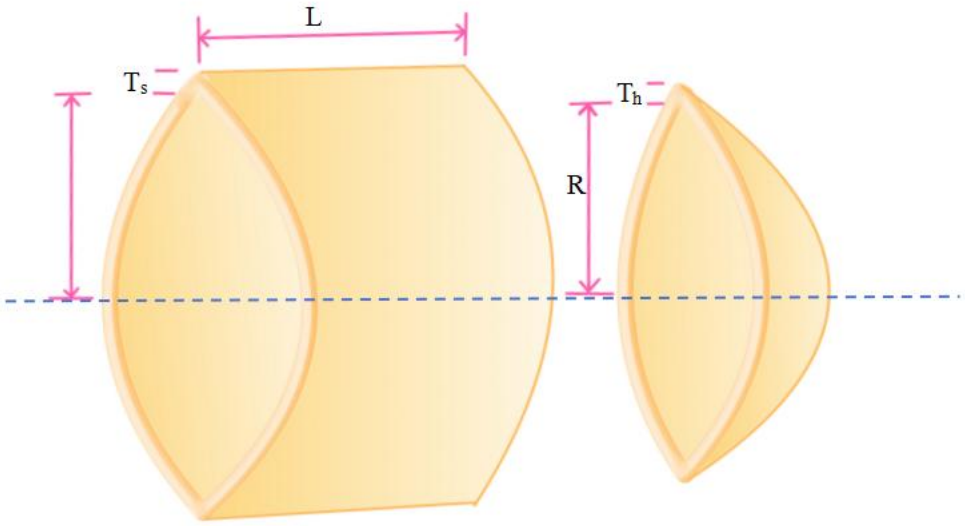

Fig.13. The pressure vessel.

In the pressure vessel design problem, the primary goal is to minimize the aggregate manufacturing cost, which encompass expenses for materials, forming, and welding. As depicted in the structure shown in **Fig. 13** Four inequality constraints govern the problem, with one of them nonlinear and the other linear. The four variables are the thickness of the shell ($x1 = Ts$), the thickness of the head ($x2 = Th$), the inner radius ($x3 = R$), and the length of the cylindrical section of the vessel ($x4 = L$). The pressure vessel problem exemplifies a mixed integer problem, with the shell and the head thickness required to be integers. At the best known feasible solution, the objective function value is approximately $f(x*) = 6059.7143$. The formulaic expression of this task is included below:

Minimize:

$$f(x) = 0.6224x_1x_3x_4 + 1.7781x_2x_3^2 + 3.1661x_1^2x_4 + 19.84x_1^2x_3 \quad (16)$$

Subject to:

$$\begin{cases} g_1(x) = -x_1 + 0.0193x_3 \le 0 \\ g_2(x) = -x_2 + 0.00954x_3 \le 0 \\ g_3(x) = -\pi x_3^2 x_4 - \frac{4}{3}\pi x_3^3 + 1296000 \le 0 \\ g_4(x) = x_4 - 240 \le 0 \end{cases} \quad (17)$$

Where:

$$Z_1 = 0.0625X_1, Z_2 = 0.0625X_2 \quad (18)$$

With bound:

$$0 \le x_1, x_2 \le 99{,}10 \le x_3, x_4 \le 200 \quad (19)$$

Table 12 Results of the pressure vessel problem.

Algorithm	x1	x2	x3	x4	F(min)
MELGWO	14.56417838	7.81910376	48.5750346	110.0684941	6.3708E+03
HSCA	16.34824438	7.753479886	51.76119076	85.00338272	6.4165E+03
GQPSO	17.70246959	9.93234651	56.74782354	53.58225003	7.3475E+03
WOA	19.25682016	23.39247769	60.76464689	30.70619347	1.2654E+04
GSA	25.71892393	46.15292088	53.3489172	100.9002616	2.3632E+04
MFO	19.84646018	10.46078889	64.63460399	12.56776309	7.3405E+03
SCHO	14.32136375	6.986479845	45.32398238	140.5592665	6.0967E+03
PO	21.2826632	9.558225727	64.53579722	13.0036261	7.5906E+03
NRBO	13.11886256	6.5	41.68173097	181.869691	6.1111E+03
CPO	27.77363381	9.962409979	64.34014245	45.36614809	1.2129E+04
HO	15.93265152	10.47862031	51.39290204	87.68190715	7.0372E+03
DLBO	**14.31564956**	**7.05620604**	**45.33453931**	**140.2929557**	**6.0912E+03**

Based on **Table 12**, we can see the outstanding performance of DLBO in optimizing manufacturing cost. The minimum objective function value $F_{min} = 6091.2$, a superior result to its competitors like, GQPSO, WOA, GSA, etc. In particular, the optimization variables of DLBO are $x_1 = 14.3156, x_2 = 7.0562, x_3 = 45.3345,$ and $x_4 = 140.293$, demonstrating the optimal capability of achieving the near-optimal results in parameter searching and reducing the manufacturing cost significantly within the design constraints. Such experimental outcomes validate the efficiency of DLBO within mixed integer optimization problems.

Further analysis also demonstrates that DLBO achieves a good balance between global exploration and local search. In contrast, the minimum objective function value of the GSA algorithm reached 2.3632×10^4, significantly higher than that of other algorithms, demonstrating a clear disadvantage in high-dimensional scenarios. However, the DLBO algorithm is able to maintain a consistently low objective function value, indicating its stronger adaptability and robustness in solving multi-constraint optimization problems. Additionally, DLBO has performed especially well in parameter x_4 with a value of 140.293, a very close value to the overall best 140.559 by SCHO, another clear evidence of DLBO's superiority and stability. In the future, we aim to further enhance the structural design of the DLBO algorithm to enhance the performance when encountering real-time or quick-response scenarios.

4.3 Multiple disc clutch brake

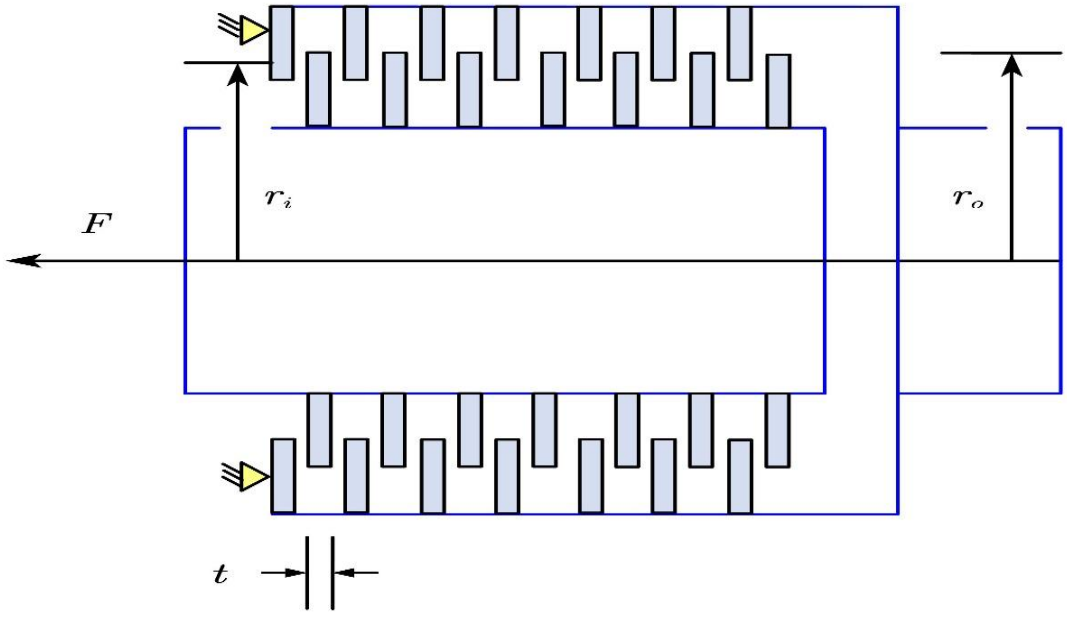

Fig. 14. Multiple disc clutch brake.

This problem is taken from. **Fig. 14** shows a multiple disc clutch brake. The objective is to minimize the mass of the multiple disc clutch brake using five discrete variables: inner radius ($r_i = 60, 61, 62, \ldots, 80$), outer radius ($r_o = 90, 91, 92, \ldots, 110$), thickness of discs ($t = 1, 1.5, 2, 2.5, 3$), actuating force ($F = 600, 610, 620, \ldots, 1000$) and number of friction surfaces ($Z = 2, 3, 4, 5, 6, 7, 8, 9$).

Table 13 Results of the multiple disc clutch brake problem.

Algorithm	x1	x2	x3	x4	x5	F(min)
MELGWO	70	90	1	169.4017128	2	2.3524E-01
HSCA	70.0520201	90.07615168	1	838.6239295	2	2.3571E-01
GQPSO	60	90	1	484.508838	2	3.3081E-01
WOA	69.99999985	90	1	273.1751498	2	2.3524E-01
GSA	76.84830372	96.38771765	1.160747791	589.4096221	2.190854199	3.0721E-01
MFO	70	90	1	999.9988162	2	2.3524E-01
SCHO	70	90	1	248.950704	2	2.3524E-01
PO	69.9996474	90	1	302.9583078	2	2.3524E-01
NRBO	70	90	1	1000	2	2.3524E-01
CPO	73.1589147	94.27023447	1.213745283	692.0396056	2.005027959	3.1591E-01
HO	45.3160422	65.31875868	0.811343428	228.2117872	1.450607792	1.0782E-01
DLBO	**69.99946182**	**90**	**1**	**735.3758436**	**2**	**2.3524E-01**

According to **Table 13**, the DLBO algorithm performs well in the mass optimization problem of multiple disc clutch brake problem. Its minimum objective function value $F_{min} = 735.3758436$ compared to 589.4096221 for GSA and 999.9988162 for MFO, demonstrating better optimization results. Particularly in comparison with MFO, the lower objective function value of DLBO indicates its advantages in efficiency and the ability to find the optimal solution.

The DLBO algorithm demonstrates stability in parameter settings, with both $x1$ and $x2$ set to 90, indicating that these parameter choices are suitable for the optimization results. All algorithms selected 1 for the x3 parameter, showing this is a universally optimal choice. These results not only prove the effectiveness of DLBO in such engineering problems but also highlight its high performance. Combined with the previously mentioned F_{min} value (minimum objective function value), DLBO shows superiority not only in absolute values but also in parameter selection, exhibiting high adaptability and stability. This further reinforces its feasibility and effectiveness in practical applications.

4.4 Robot Gripper Problem

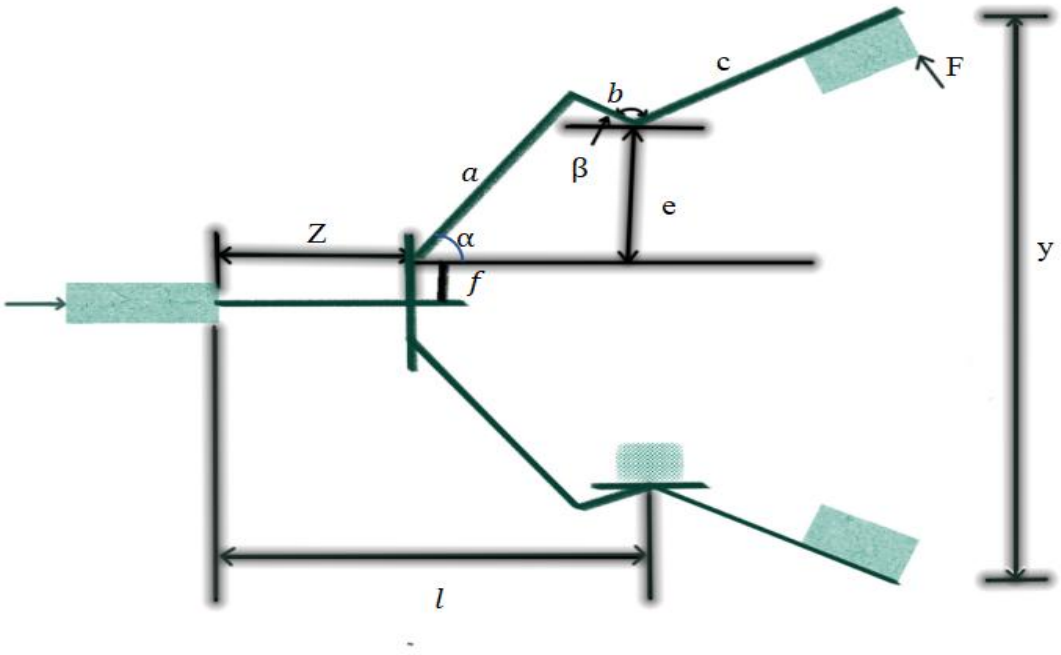

Fig. 15. The robot gripper.

The optimization of the robot gripper aims to reduce the discrepancy between the highest and lowest forces that the gripper can exert. This reduction is accomplished through manipulating various displacements at the end position of the gripper. We can see from **Fig. 15** that, it encompasses six distinct factors: the lengths of the linkages denoted as a, b, c, the vertical displacement e, the vertical distance f, the horizontal distance l, and the geometric angle δ. The formulaic expression of the problem in mathematics is shown as follows.

$$x^* = (0.7782, 0.3847, 40.3201, 199.9975) \tag{20}$$

Consider:

$$x = [x_1, x_2, x_3, x_4, x_5, x_6, x_7] = [a, b, c, e, f, l, \delta] \tag{21}$$

Minimize:

$$f(x) = -min(z)F(x, z) + max(z)F_k(x, z) \tag{22}$$

$$
\begin{aligned}
&g_1(x) = -Y_{\min} + Y(x, Z_{\max}) \le 0, g_2(x) = -Y((x), Z_{\max}) \le 0, \\
&g_3(x) = Y_{\max} - Y((x), 0) \le 0, g_4(x) = Y((x), 0) - Y_G \le 0, \\
&g_5(x) = l^2 + e^2 - (a+b)^2 \le 0, g_6(x) = b^2 - (a-e)^2 - (I - Z_{\max})^2 \le 0, \\
&g_7(x) = Z_{\max} - l \le 0,
\end{aligned} \tag{23}
$$

Where:

$$
\begin{aligned}
a = cos_{-1}\left(\frac{a^2 + g^2 - b^2}{2ag}\right) + \phi, \quad g = \sqrt{e^2 + (z-l)^2}, \beta \\
= cos_{-1}\left(\frac{b^2 + g^2 - a^2}{2ag}\right) - \phi, \phi = tan_{-1}\left(\frac{e}{l-z}\right), Y(x,z) \\
= 2(f + e + c\, sin(\beta + \delta)), F_k = \frac{Pb\, sin(a+\beta)}{2c\, cos(\alpha)}
\end{aligned} \tag{24}
$$

Parameters ranges:

$$
\begin{aligned}
&Y_{\min} = 50, Y_{\max} = 100, Y_G = 150, Z_{\max} = 100, P = 100 \\
&0 \le e \le 50, 100 \le c \le 200, 10 \le f \\
&a, b \le 150, 1 \le \delta \le 3.14, 100 \le l \le 300
\end{aligned} \tag{25}
$$

Table 14 Results of the robot gripper problem.

Algorithm	x1	x2	x3	x4	x5	x6	x7	F(min)
MELGWO	150	150	200	0	93.033386	100	2.032287833	4.2893E+00
HSCA	142.6927365	91.5407818	159.7020357	48.47945605	112.3006135	137.557484	2.977070432	5.1701E+00
GQPSO	99.53227222	69.64785	100	5.073036444	10	152.0468752	1	8.6320E+18
WOA	150	150	199.4589156	0	13.13765619	100	1.636710694	4.3010E+00
GSA	66.64512142	71.45058037	144.4034349	19.99356472	84.02983416	187.770426	2.32118677	1.6482E+24
MFO	150	136.4199321	100	4.451904853	54.34248199	182.1440032	2.202578486	7.8315E+00
SCHO	107.2247012	104.5149952	134.2671065	2.207076454	12.05364388	107.038258	1.634805919	6.1253E+00
PO	149.8266086	149.6972376	186.6241281	19.39118932	10.02653747	246.8626379	2.375432942	4.3584E+01
NRBO	150	141.78661	153.9717344	6.681301054	36.17254458	140.7768	1.860247679	4.2005E+00
CPO	128.5626027	99.41184701	102.0895434	26.08923952	56.47658431	164.0796399	2.706611798	1.8234E+01
HO	149.9672407	121.4001498	124.5782874	12.55610628	114.9139943	192.4077175	2.985808443	7.0817E+00
DLBO	**143.727077**	**123.4342533**	**165.8847288**	**19.61162725**	**141.5523505**	**120.820602**	**2.693277983**	**3.8939E+00**

From **Table 14**, DLBO achieves minimum objective function value $F_{min} = 3.8939$, the lowest value within the table. This indicates that the DLBO algorithm performs exceptionally well in optimizing the parameter settings of robot grippers, effectively reducing the force disparity. From the parameter selection perspective, DLBO selects 143.72077, 123.4342533, 165.8847288 for x_1, x_2, and x_3 correspondingly. These parameters are shorter or more optimal compared to the choices of many other algorithms. For example, MELGWO selects 150, 150, 200 respectively. This indicates that DLBO optimizes the force transmission efficiency while reducing the structural size. For the angular parameters, DLBO chooses 96.1162275, 141.5523505, 120.82602, 2.693927983 for x_4 to x_7 respectively, demonstrating its precision and efficiency in adjusting angles to meet force transmission requirements.

In summary, DLBO has delivered excellent results in numerical optimization, especially when working with large-scale test examples such as the CEC2017 benchmark suite, which includes complex problems like the rotated high-dimensional functions, and the CEC2022 benchmark suite, known for its challenging multimodal functions. Its parameter selection reflects a deep and strong understanding of the underlying physical model of the problem. This performance demonstrates the effectiveness of the DLBO algorithm in addressing complex engineering optimization problems, especially in scenarios requiring precise control and efficient force transmission. Future research and optimization of the DLBO algorithm's structure can make it more adaptable and effective across a variety of real-world scenarios.

5 The application of Graph Convolutional Networks optimized by deep learning

In recent years, Graph Convolutional Networks (GCNs) have proven to be highly effective in working with non-Euclidean data structures, such as social networks, citation networks, and biological datasets. This paper introduces an optimized GCN model for the task of breast cancer data classification. To improve the model's performance, multiple optimization algorithms, including DLBO, are chosen to fine-tune key hyperparameters such as the number of hidden nodes and the learning rate. This approach creates a more efficient model that is specifically designed to better understand and work with the unique underlying structure of the dataset.

5.1 Data Preprocessing

In this study, we used a medical dataset of breast cancer patients who had surgery at Shaoxing People's Hospital between 2010 and 2020, and the relevant data can be found in the supplementary materials. To ensure data integrity and accuracy, patients with incomplete records or those lost to follow-up were excluded. The

dataset used in this study is loaded from an Excel file containing features and labels. We have chosen 80% of the data as a training set and the remaining 20% as a test set from each dataset, ensuring that the dependent variable is well represented in both sets. The classification error on the test set was used as the objective function, with the chosen feature subsets acting as independent variables. The processing steps are as follows:

- **Shuffling:** The dataset is randomized to remove any inherent order and avoid bias in model training.
- **Splitting:** The dataset is divided into training and test sets using stratified sampling, ensuring that both sets maintain the original class distribution.
- **Normalization:** Feature scaling is performed using the map minmax function, which normalizes the feature values into the range [0, 1].

Let $X \in R^{n\times m}$ represent the feature matrix, where n is the number of samples and m is the number of features. The corresponding label vector $Y \in R^{n\times 1}$ represents the class labels. After normalization, the data X is transformed to $X' \in [0,1]^{n\times m}$.

5.2 Graph Convolutional Network (GCN) Model

GCNs extend traditional convolutional neural networks (CNNs) to graph-structured data by defining convolutions on graphs. In this model, the graph structure is represented by an adjacency matrix $A \in R^{m\times m}$, constructed from the pairwise Spearman correlation coefficients between features. The GCN model learns feature representations by leveraging the graph structure in a layer-wise fashion as shown in **Fig. 16**.

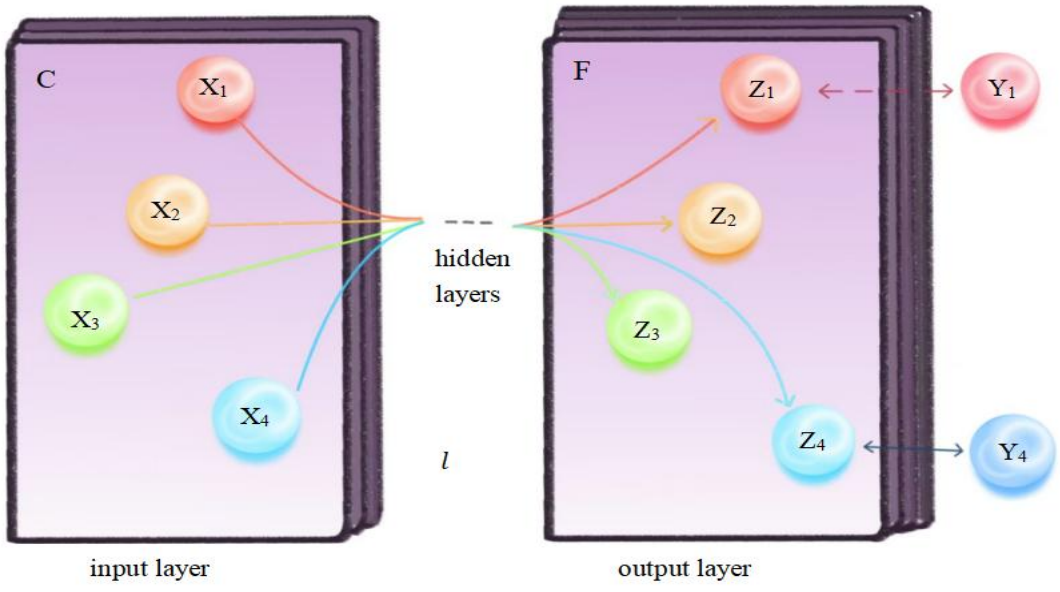

Fig. 16. Graph Convolutional Network.

5.2.1 Model Architecture

1) **Graph Convolutional Layer 1:** The first graph convolutional layer computes feature representations by applying a linear transformation to the input features and propagating them through the graph defined by *A*. The operation is given by:

$$Z_2 = Re\,L\,U(AXW_1) + X \tag{26}$$

where $W_1 \in R^{m \times h}$ represents the weight matrix of the layer, and *h* is the number of hidden nodes.

2) **Graph Convolutional Layer 2:** A second graph convolutional layer refines the feature representations:

$$Z_3 = Re\,L\,U(AZ_2W_2) + Z_2 \tag{27}$$

where $W_2 \in R^{h \times h}$ is the weight matrix for this layer.

3) **Classification Layer:** Finally, a softmax function is applied to the output layer to generate class probabilities:

$$Z_5 = soft\,max(W_4^T Z_4) \tag{28}$$

where $W_4 \in R^{h \times c}$ is the weight matrix, and *c* is the number of output classes.

5.2.2 Loss Function

The model's loss function is based on cross-entropy, which is commonly used in classification problems. Given the true class labels *T* and the predicted probabilities *Y* , the cross-entropy loss is defined as:

$$\mathscr{L} = -\sum_{i=1}^{n} T_i\,log(Y_i) \tag{29}$$

where *Ti* is the one-hot encoded vector for the true label, and *Yi* is the predicted probability for the *i*-th sample.

5.2.3 Optimization Algorithms

The hyperparameters of the GCN model, particularly the number of hidden nodes and the learning rate, are optimized using multiple optimization algorithms. The objective function, defined as the classification error on the test set, is minimized. The algorithms employed include: Modified Grey Wolf Optimizer (MELGWO), Global Quantum Particle Swarm Optimization (GQPSO), Whale Optimization Algorithm (WOA), Gravitational Search Algorithm (GSA), Moth Flame Optimizer (MFO), Simplified Chimp Optimization (SCHO), Particle

Optimization (PO), Nature-Inspired Random Bat Algorith (NRBO), Cooperative Particle Optimization (CPO), Harmony Search Optimization (HO), main algorithm Dead Leaf Butterfly Optimization (DLBO).

The optimization process searches for the optimal combinations of the hyperparameters $\boldsymbol{x} = [h, \eta]$, where h stands for the number of hidden nodes, and η represents the learning rate, by solving the following minimization problem:

$$Min_x \varepsilon(x) \tag{30}$$

where $\varepsilon(\boldsymbol{x})$ represents the classification error on the test set. The algorithm iterates over the following search space for hyperparameters:

1) **Number of Hidden Nodes (h):**

$$h \in \{4,8,12,16,20,24,28,32,36,40,44,48,52,56,60,64\} \tag{31}$$

2) **Learning Rate (η):**

$$\eta \in \{0.01,0.03,0.001,0.003,0.0001,0.0003,0.00001,0.00003,0.00003,0.000001,0.000003\} \tag{32}$$

These algorithms explore the hyperparameter space by iterating over different combinations of h and η, with the goal of minimizing classification error on the testing dataset. The multi-objective optimization framework makes sure that the GCN model is fine-tuned for both performance and generalization.

5.2.4 Training Process

The model is trained using the Adam optimizer, an adaptive optimization method that dynamically adjusts the learning rate. The update rules for the weights are given by:

$$\theta_t = \theta_{t-1} - \frac{\alpha}{\sqrt{v_t}+\int} m_t \tag{33}$$

where α stands for the learning rate, mt and v_t represent the first and second moment estimates of the gradients, and ϵ denotes a small constant for numerical stability. The training process runs for a total of 1000 epochs. The effectiveness of the model is assessed using the test set, and the results are recorded for further analysis.

5.2.5 Performance metrics of the GCN model

In the experiments, the performance of the GCN model is evaluated using metrics like Accuracy, Sensitivity (Recall), and others, offering a comprehensive view of the model's effectiveness. Accuracy measures the overall proportion of correct classifications made by the model, reflecting its classification capability. Sensitivity (Recall), on the other hand, focuses on how well the model is able to identify positive instances, which is particularly important when dealing with imbalanced datasets. By analyzing these metrics, we can have better understanding about the performance of the GCN model in various application scenarios and identify potential areas where it can be improved.

- **Accuracy:** The proportion of correctly classified samples. It is calculated as:

$$Accuracy = \frac{TP+TN}{TP+TN+FP+FN} \times 100 \tag{34}$$

where *TP*, *TN*, *FP*, and *FN* stand for true positives, true negatives, false positives, and false negatives, correspondingly.

- **Sensitivity (Recall):** The ability to correctly identify positive samples:

$$Sensitivity = \frac{TP}{TP+FN} \times 100 \tag{35}$$

- **Specificity:** The ability to correctly identify negative samples:

$$Specificity = \frac{TN}{TN+FP} \times 100 \tag{36}$$

- **Matthews Correlation Coefficient (MCC):** A balanced measure considering both true and false positives and negatives:

$$MCC = \frac{TP \times TN - FP \times FN}{\sqrt{(TP+FP)(TP+FN)(TN+FP)(TN+FN)}} \tag{37}$$

Experimental results including accuracy, sensitivity, specificity, and MCC, are saved in Excel files for each optimization algorithm.

This study demonstrates the effectiveness of applying GCNs to breast cancer classification, using various optimization algorithms to fine-tune hyperparameters. The combination of GCN and DLBO provides a robust model that efficiently handles the dataset, yielding high accuracy, sensitivity, and specificity. Future work could explore more sophisticated graph construction techniques and deeper GCN architectures for improved performance.

5. 3 Feature of Breast Cancer Breast Cancer dataset

The features utilized from the breast cancer dataset include Age, ER (Estrogen Receptor), PR (Progesterone Receptor), HER2 (Human Epidermal Growth Factor Receptor 2), p53, Ki67, Long Diameter, Short Diameter, Lymph Node Metastasis, Total Lymph Node, and Vascular Invasion. The classification variable in the Breast Cancer Dataset focuses on whether the patient survived during the follow-up period. **Table 15** presents the selected features from the two breast cancer datasets along with their definitions.

Table 15 Feature of Breast Cancer Dataset and their Basic conception.

Feature	Basic conception
Age	The age of the patient at the time of diagnosis.
ER (Estrogen Receptor)	The presence of estrogen receptors on tumor cells, indicating hormone sensitivity.
PR (Progesterone Receptor)	The presence of progesterone receptors on tumor cells, often used alongside ER to assess hormone receptor status.
HER2	A protein that promotes cell growth, with overexpression linked to more aggressive breast cancer.
p53	A tumor suppressor gene mutation often associated with cancer progression.
Ki67	A marker for cell proliferation, used to evaluate tumor growth activity.
Pathological Grade	The degree of differentiation of tumor cells, indicating tumor aggressiveness.
Long Diameter	The longest measurable dimension of the tumor.
Short Diameter	The shortest measurable dimension of the tumor.
Lymph Node Metastasis	The spread of cancer cells to nearby lymph nodes.
Total Lymph Node	The total number of lymph nodes assessed during diagnosis or surgery.
Vascular Invasion	The spread of tumor cells into blood vessels or lymphatics.

5. 4 Classification and clinical significance of Breast Cancer Staging and Molecular Subtypes

Breast cancer diagnosis and treatment rely on precise classification systems that guide clinical decision-making. This section focuses on the two critical aspects: Breast Cancer TNM Staging System and Mechanisms of Metastasis and Characteristics and Treatment Strategies of Breast Cancer Molecular Subtypes.

5. 4. 1 Breast Cancer TNM Staging System and Mechanisms of Metastasis

TNM refers to the size of the primary tumor and whether it has invaded nearby tissues. As shown in Fig. 10, It ranges from T0 (no evidence of a primary tumor) to T4 (large tumor or one that has grown into nearby structures). The TNM staging system is a standardized method to assess breast cancer progression based on tumor size (T), lymph node involvement (N), and metastasis (M).

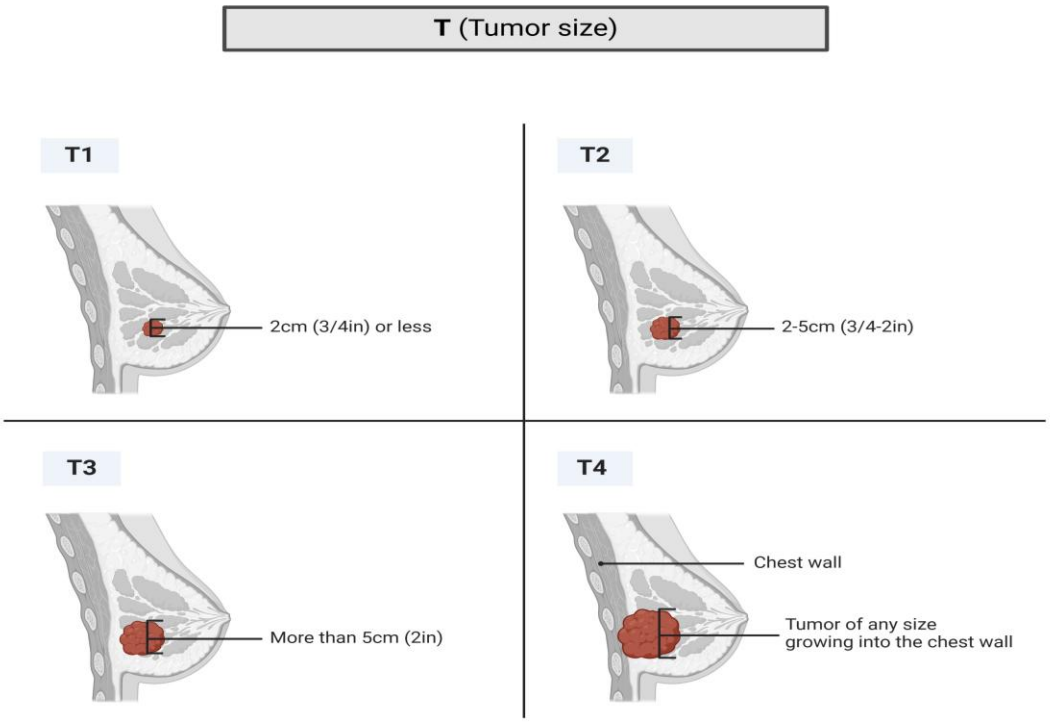

Fig. 17. The overview of Tumor size.

- **Tumor Size (T):** T describes the size of the primary tumor and the extent of its invasion, which is illustrated in **Fig. 17**. It is classified as follows

1) T1: Tumor size is 2 cm (¾ inch) or smaller.
2) T2: Tumor size ranges from 2 to 5 cm (¾–2 inches).
3) T3: Tumor size exceeds 5 cm (2 inches).
4) T4: The tumor invades the chest wall or skin, regardless of size, indicating advanced local progression.

- **Lymph Node Involvement (N):** As shown in **Fig. 18**, N describes whether the cancer cells have spread to the regional lymph nodes and the extent of such spread:

1) N0: Cancer has not spread to axillary lymph nodes.
2) N1–N3: Cancer has spread to one or more lymph nodes, reflecting a more advanced stage and a higher likelihood of systemic dissemination.

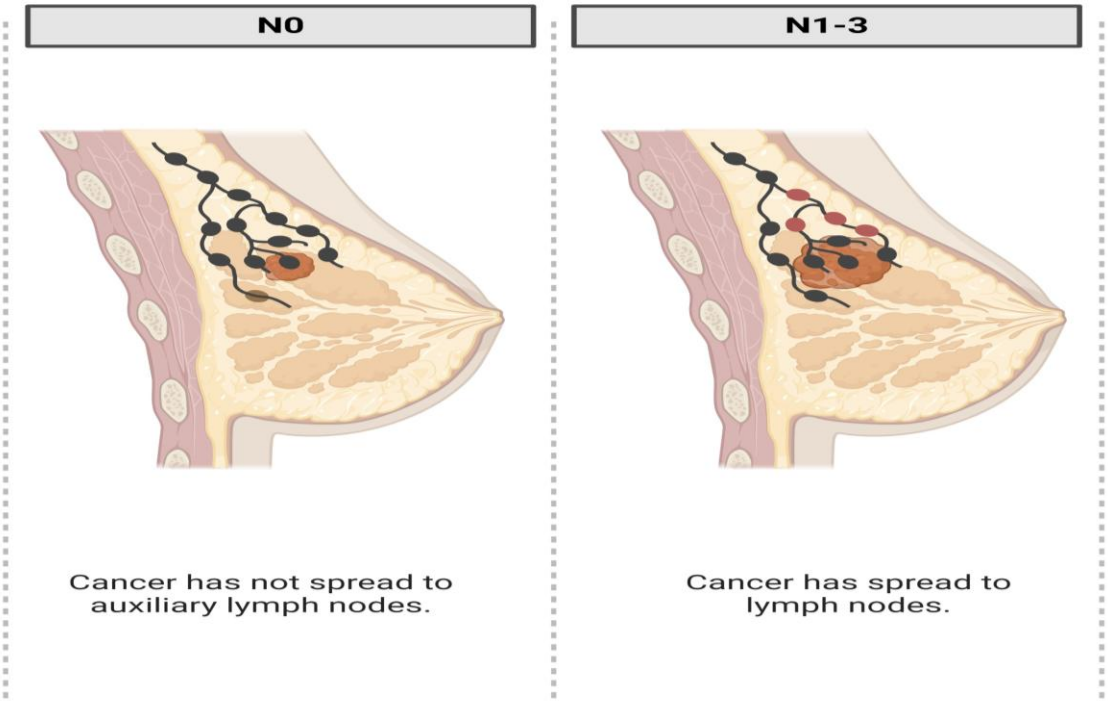

Fig. 18. The overview of Lymph Node Involvement (N).

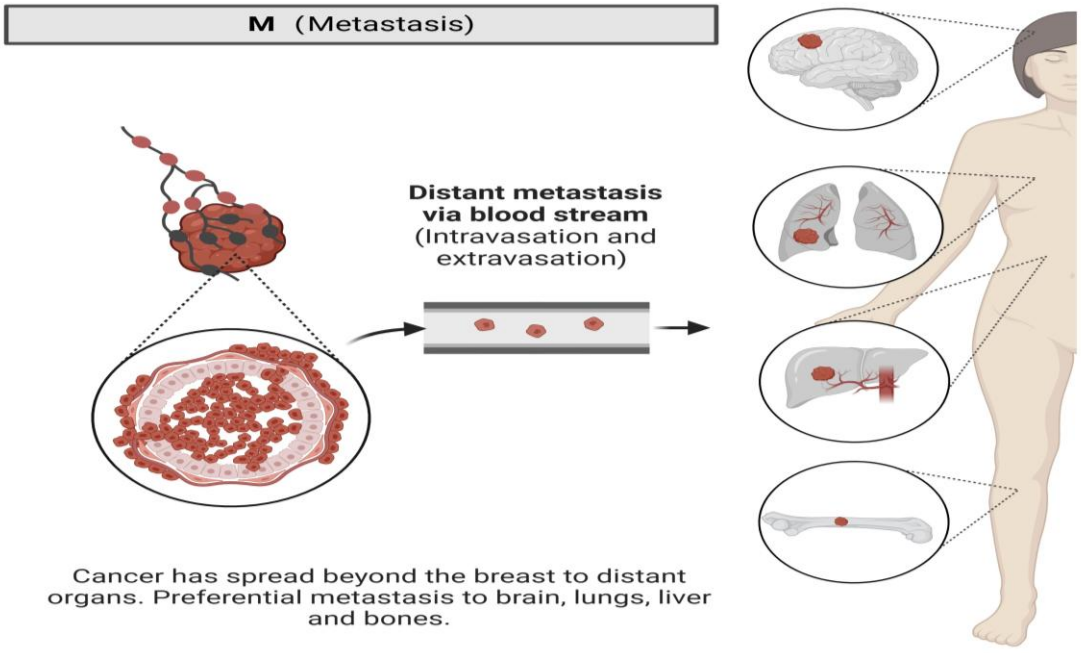

Fig. 19. The description of Metastasis (M).

Metastasis (M): The "M" category represents the spread of cancer beyond the breast and regional lymph nodes to distant organs, such as the brain, lungs, liver, or bones. This process, as presented in **Fig. 19**, involves intravasation (entry into the bloodstream) and extravasation (exit from the bloodstream to distant tissues). Metastasis is the most critical factor in determining prognosis and treatment strategy.

5. 4. 2 Characteristics and Treatment Strategies of Breast Cancer Molecular Subtypes

The section focuses on the molecular subtypes of breast cancer, along with their clinical characteristics, treatment strategies, and prognoses. The detailed introduction is presented in **Fig. 20**. Based on hormone receptor status and gene expression profiles, breast cancer can be classified into four major molecular subtypes:

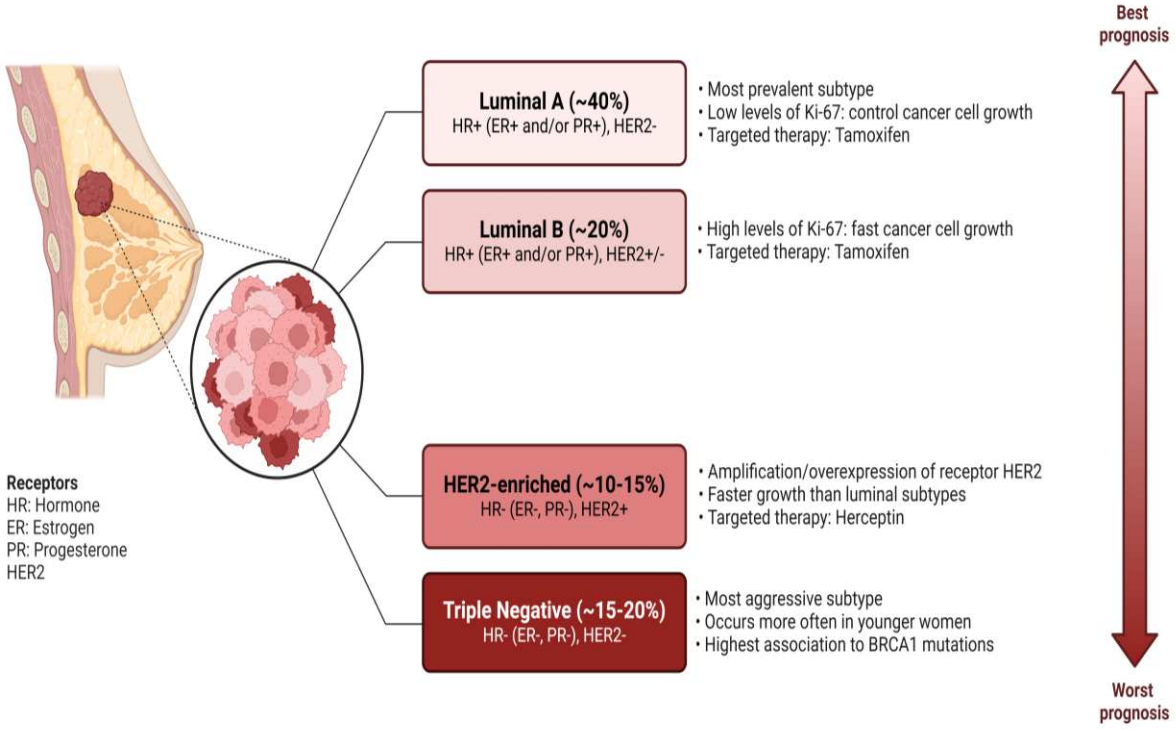

Fig. 20. Classification and Clinical Characteristics of Breast Cancer Molecular Subtypes.

- **Luminal A (Approximately 40%)**

1) Characteristics: This is the most common subtype of breast cancer, characterized by hormone receptor positivity (HR+, including estrogen receptor ER+ and/or progesterone receptor PR+) and HER2 negativity (HER2-).
2) Proliferation Rate: Low Ki-67 levels, indicating slower cell proliferation.
3) Treatment Strategy: Mainly treated with endocrine therapy (e.g., Tamoxifen) to control tumor growth.
4) Prognosis: Best prognosis among all subtypes.

- **Luminal B (Approximately 20%)**

1) Characteristics: Similar to Luminal A, it is HR+ but has higher Ki-67 levels, indicating higher proliferative activity. HER2 status can be either positive or negative (HER2+/-).
2) Treatment Strategy: Primarily treated with endocrine therapy (e.g., Tamoxifen). Due to its higher proliferation rate, chemotherapy or targeted therapy may also be required.
3) Prognosis: Slightly worse than Luminal A but still better than HER2-enriched and triple-negative subtypes.

- **HER2-Enriched (Approximately 10%-15%)**

1) Characteristics: HER2-positive (HER2+), hormone receptor-negative (HR-, i.e., ER- and PR-). Tumor cells in this subtype tend to grow and divide more rapidly.
2) Treatment Strategy: Mainly treated with anti-HER2 targeted therapies (e.g., Trastuzumab/Herceptin), combined with chemotherapy to inhibit tumor progression.
3) Prognosis: With effective targeted therapy, prognosis is relatively favorable. However, without timely treatment, disease progression is rapid.

- **Triple-Negative Breast Cancer (Approximately 15%-20%)**

1) Characteristics: Lacks hormone receptors and HER2 expression (HR-, HER2-). This subtype is highly aggressive and often seen in younger women. It is also strongly associated with BRCA1 gene mutations.
2) Treatment Strategy: Due to the absence of therapeutic targets, chemotherapy is currently the only available treatment, though efficacy is limited.
3) Prognosis: The worst prognosis among all subtypes, with a high risk of recurrence and metastasis.

- **Prognostic Differences Among Subtypes:** Luminal A has the best prognosis, while the prognosis worsens progressively across subtypes. Triple-negative breast cancer has the poorest prognosis, making it a major focus of research and treatment challenges.

- **Clinical Significance:** This classification underscores the importance of molecular subtypes in the diagnosis and treatment of breast cancer. Precision classification based on molecular subtypes enables the selection of targeted therapies, improving treatment outcomes and patient survival rates.

5. 3 Analysis of DLBO-GCN hyperparameter experimental results

Table 16 Comparison of Results between DLBO and eleven Other Algorithms on the Breast Cancer Dataset.

Algorithm	ACC	Sensitivity	Specificity	MCC
MELGWO	0.88	1	0.76	0.78
HSCA	0.9	1	0.8	0.82

GQPSO	0.9	1	0.8	0.82
WOA	0.86	1	0.72	0.75
GSA	0.58	0.48	0.68	0.16
MFO	0.9	1	0.8	0.82
SCHO	0.9	1	0.8	0.82
PO	0.9	1	0.8	0.82
NRBO	0.88	1	0.76	0.78
CPO	0.88	1	0.76	0.79
HO	0.9	1	0.8	0.82
DLBO	**0.9**	**1**	**0.8**	**0.82**

In the Breast Cancer Dataset, the survival status of patients during follow-up, categorized as either deceased or survived, is selected as the primary outcome. Features that significantly impact patient survival are identified for further analysis. **Table 16 and Fig. 13** demonstrate the accuracy results of eight algorithms on Breast Cancer Dataset. The DLBO algorithm demonstrates exceptional performance, achieving the highest results in accuracy, sensitivity, specificity, and MCC. Only GSA lagged behind other algorithms in the analysis. This evaluation highlights the DLBO method's outstanding predictive capabilities across all metrics, showcasing its strong competitive advantage over other algorithms.

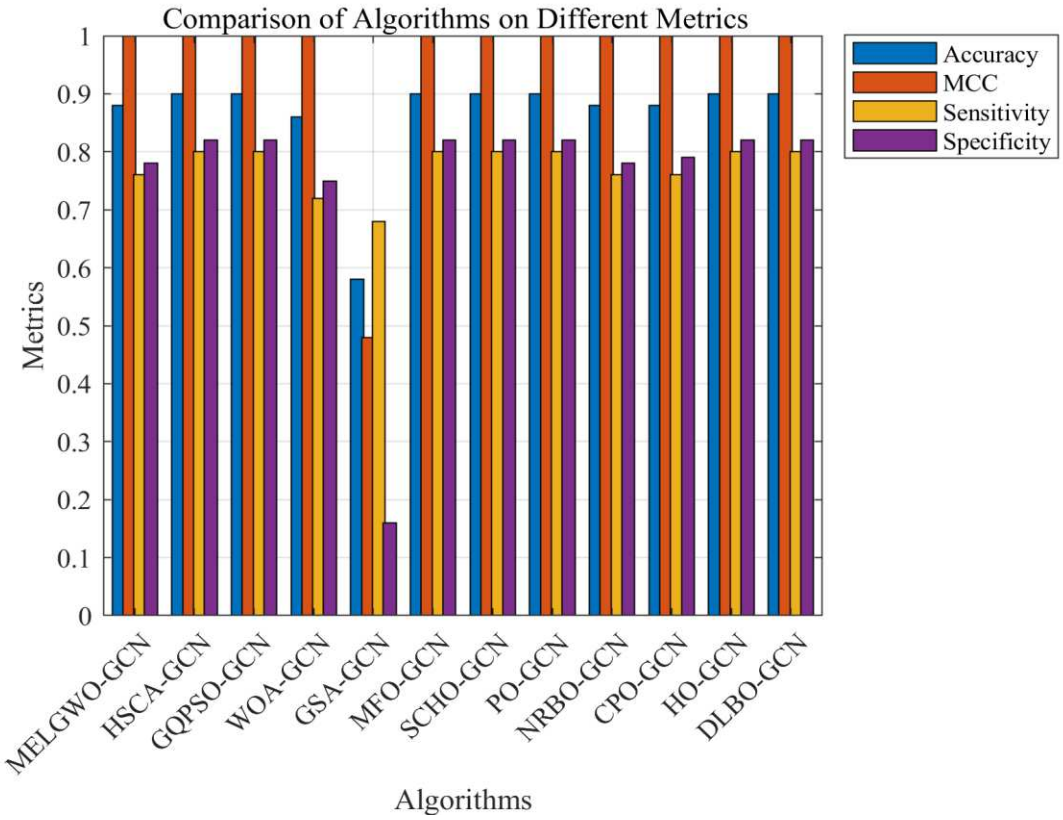

Fig. 13. Feature selection results of 12 algorithms on the Breast Cancer Dataset.

6.Conclusion

This paper introduces a new metaheuristic algorithm called the Dead Leaf Butterfly Optimizer (DLBO), inspired by the color changes, development, and migration behaviors of dead leaf butterflies. DLBO algorithm effectively combines global and local search methods, with a balanced mechanism that starts with the comprehensive exploration of the solution space and later focuses on exploiting promising regions to improve solution quality. Experiments built upon the breast cancer dataset clearly demonstrate that DLBO is able to significantly enhance the prediction performance of the GCN model, therefore improving the accuracy of feature extraction and classification for such disease.

In addition, DLBO is successful in multiple engineering tasks, such as the aforementioned compression spring design, pressure vessel design, multi-disc clutch brake design, and robot gripper optimization. The results demonstrate that DLBO is able to offer great efficiency and advantages by providing high-quality solutions for complex engineering design challenges. This further emphasizes DLBO's broad applicability and potential in the field of engineering optimization. However, DLBO presented limited improvement on specific extreme unimodal functions (e.g., F3 and F4 in CEC2017, F1 and F2 in CEC2022), possibly due to the large flat regions

in such test functions, which stagnate the optimization process to and reduce the exploration capability in the solution space thoroughly. Also, DLBO's computational complexity and parameter tuning still require optimization, particularly in application scenarios where real-time response is needed.

While DLBO has shown great success in solving complex engineering and medical problems, it still has some weaknesses and limitations. For example, DLBO may face high computational costs when dealing with high-dimensional or highly complex problems, leading to a decrease in optimization efficiency. Future research could improve DLBO's global search capability by combining it with mechanisms from other optimization algorithms, such as hybrid strategies with genetic algorithms or particle swarm optimization. Additionally, expanding DLBO into binary and multi-objective versions, or integrating it with other machine learning models, could enable its application to a wider range of challenges, such as image processing and natural language processing, thus promoting its development and innovation across broader application domains.

Declarations

Ethics approval and consent to participate

This study was conducted in compliance with all relevant ethical guidelines and regulations. All experimental protocols involving human participants and/or human tissue samples were reviewed and approved by the Ethics Committee of Jinhua Municipal Central Hospital (Approval Number: (Research)-2022-Ethical Review-253, Date of Approval: 2024-8-30).

Informed consent was obtained from all participants or, where applicable, their legal guardians prior to participation in the study. Consent forms included detailed information about the study objectives, procedures, potential risks, and the voluntary nature of participation, with a clear statement that participants had the right to withdraw from the study at any time without penalty.

Consent for publication

All authors have consented to the publication of this manuscript.

Availability of data and material

Data and materials are provided within the manuscript or supplementary information files

Funding

No funding was received for this research.

Conflict of Interest

On behalf of all authors, the corresponding author states that there is no conflict of interest.

Authors' contributions

D.W. and K.O. contributed equally as the principal leaders of the research, overseeing the overall study design and methodology. D.W. took the lead in conceptualizing the optimization algorithm, while K.O. provided substantial guidance on the mathematical and computational aspects. M.W., X.S, J.C., J.W., W.X., M.Q. and S.F. contributed to data collection, analysis, and interpretation, while K.O. also supervised the entire project. All authors reviewed and approved the final manuscript.

Reference

1. Zhang, Y., X. Li, and M. Wang, *Advances in optimization algorithms.* Journal of Optimization Theory and Applications, 2020. **184**(2): p. 345-359.
2. Beheshti, Z. and S.M.H. Shamsuddin, *A review of population-based meta-heuristic algorithms.* International Journal on Advanced Science, Engineering and Information Technology, 2013. **5**(1): p. 1-35.
3. Yang, M., S. Sharma, and F. Jiang, *A new approach to system design optimization of underwater gliders.* IEEE/ASME Transactions on Mechatronics, 2022. **27**(5): p. 3494-3505.
4. Sharma, S., F. Jiang, and L. Bai, *mLBOA: A Modified Butterfly Optimization Algorithm with Lagrange Interpolation for Global Optimization.* Journal of Bionic Engineering, 2022. **19**(4): p. 1161-1176.
5. Wang, J., X. Liu, and Y. Chen, *Applications of Metaheuristic Algorithms in Bioinformatics.* Bioinformatics and Computational Biology, 2021. **39**(2): p. 112-130.
6. Emam, M.M., E.H. Houssein, and R.M. Ghoniem, *A modified reptile search algorithm for global optimization and image segmentation: Case study brain MRI images.* Computers in Biology and Medicine, 2023. **152**: p. 106404.
7. Johnson, R. and L. Wang, *Gradient-based algorithms for optimization.* International Journal of Computational Science, 2018. **31**(5): p. 899-912.
8. Van Den Berg, E. and M.P.J. Friedlander, *Probing the Pareto frontier for basis pursuit solutions.* SIAM Journal on Scientific Computing, 2009. **31**(2): p. 890-912.
9. Houssein, E.H., M.M. Emam, and R.M. Ghoniem, *Boosted sooty tern optimization algorithm for global optimization and feature selection.* Expert Systems with Applications, 2023. **213**: p. 119015.

10. Hinton, G.E. and R.R.J. Salakhutdinov, *Reducing the dimensionality of data with neural networks.* Science, 2006. **313**(5786): p. 504-507.
11. Yang, Y., S.C. Chu, and P.W. Tsai, *Cooperative multi-population Harris Hawks optimization for many-objective optimization.* Complex & Intelligent Systems, 2021. **8**(4): p. 3299-3332.
12. Mirjalili, S. and A. Lewis, *The Whale Optimization Algorithm.* Advances in Engineering Software, 2020. **95**: p. 51-67.
13. Smith, J. and D. Lee, *Linear programming and its applications.* Algorithmic Studies, 2019. **45**(4): p. 123-135.
14. Kim, H. and S. Park, *Dynamic programming techniques in optimization.* Journal of Computational Methods, 2021. **58**(1): p. 67-84.
15. Huang, M., J. Lin, and H. Tang, *Metaheuristic algorithms in manufacturing optimization.* Journal of Manufacturing Systems, 2023. **65**(3): p. 210-225.
16. Liu, J., X. Yu, and Y. Li, *Enhanced Butterfly Optimization Algorithm for Large-Scale Optimization Problems.* Journal of Bionic Engineering, 2021. **19**(2): p. 554-570.
17. Simon, D., *Biogeography-based optimization.* IEEE Transactions on Evolutionary Computation, 2008. **12**(6): p. 702-713.
18. Beyer, H.G. and H.P. Schwefel, *Evolution strategies–a comprehensive introduction.* Natural Computing, 2002. **1**: p. 3-52.
19. Storn, R. and K. Price, *Differential Evolution – A Simple and Efficient Heuristic for global Optimization over Continuous Spaces.* Journal of Global Optimization, 1997. **11**(4): p. 341-359.
20. Glover, F., *Future paths for integer programming and links to artificial intelligence.* Computers & Operations Research, 1986. **13**(5): p. 533-549.
21. Kennedy, J. and R. Eberhart. *Particle Swarm Optimization*. 1995.
22. Dorigo, M. and T. Stützle, *Ant Colony Optimization*. 2004: MIT Press.
23. Yang, M., S. Sharma, and F. Jiang, *Performance Comparison of Swarm Intelligence Algorithms.* Advanced Computational Intelligence, 2021. **30**(4): p. 345-359.
24. Mirjalili, S., S.M. Mirjalili, and A. Lewis, *Grey Wolf Optimizer: Theory, Literature Review, and Application in Computational Fluid Dynamics Problems.* Nature-Inspired Optimizers: Theories, Literature Reviews and Applications, 2016: p. 87-105.
25. Chen, L., P. Zhao, and Q. Xu, *Optimization algorithms in transportation and logistics.* Transportation Research Part B: Methodological, 2023. **48**(1): p. 95-110.
26. Hashim, F.A., E.H. Houssein, and R.M. Ghoniem, *Henry gas solubility optimization: A novel physics-based algorithm.* Future Generation Computer Systems, 2019. **101**: p. 646-667.

27. Zhang, Z., W. Yu, and H. Wang, *Towards augmented kernel extreme learning models for bankruptcy prediction: Algorithmic behavior and comprehensive analysis.* Neurocomputing, 2021. **430**: p. 185-212.
28. Chen, L., P. Zhao, and Q. Xu, *Benchmarking Optimization Algorithms: A Review.* Journal of Computational Methods, 2023. **58**(1): p. 67-84.
29. Su, H., T. Zhou, and Y. He, *RIME: A physics-based optimization.* Neurocomputing, 2023. **532**: p. 183-214.
30. Rahman, C.M., *Group learning algorithm: a new metaheuristic algorithm.* Neural Computing and Applications, 2023. **35**(19): p. 14013-14028.
31. Dorigo, M. and T. Stützle, *Ant Colony Optimization*. 2019: MIT Press.
32. Bonabeau, E., M. Dorigo, and G. Theraulaz, *Swarm Intelligence: From Natural to Artificial Systems*. 1999: Oxford University Press.
33. Blum, C. and X. Li, *Swarm Intelligence in Optimization.* Natural Computing, 2008. **7**(3): p. 231-257.
34. Dorigo, M., M. Birattari, and T. Stutzle, *Ant Colony Optimization: Artificial Ants as a Computational Intelligence Technique.* IEEE Computational Intelligence Magazine, 2006. **1**(4): p. 28-39.
35. Shi, Y. and R.C. Eberhart. *A Modified Particle Swarm Optimizer*. 1998.
36. Eberhart, R.C. and Y. Shi, *Particle Swarm Optimization: Developments, Applications and Resources.* Proceedings of IEEE International Conference on Evolutionary Computation, 2001. **1**: p. 81-86.
37. Yang, X.S., et al., *Swarm Intelligence and Bio-Inspired Computation: Theory and Applications.* Elsevier, 2021. **25**(2): p. 110-119.
38. Wolpert, D.H. and W.G. Macready, *No Free Lunch Theorems for Optimization.* IEEE Transactions on Evolutionary Computation, 1997. **1**(1): p. 67-82.
39. Ho, Y.C. and D.L. Pepyne, *Simple Explanation of the No-Free-Lunch Theorem and Its Implications.* Journal of Optimization Theory and Applications, 2002. **115**(3): p. 549-570.
40. Jones, D.R., C.D. Perttunen, and B.E. Stuckman, *Lipschitzian Optimization without the Lipschitz Constant.* Journal of Optimization Theory and Applications, 2001. **79**(1): p. 157-181.
41. Smith, J., D. Lee, and H. Chen, *Bio-Inspired Optimization Algorithms.* Computational Intelligence, 2022. **38**(4): p. 567-582.
42. Li, H. and T. Zhang, *Performance Comparison of Swarm Intelligence Algorithms.* Advanced Computational Intelligence, 2020. **30**(4): p. 345-359.
43. Chen, L., P. Zhao, and Q. Xu, *Optimization algorithms in transportation and logistics.* Transportation Research Part B: Methodological, 2022. **48**(1): p. 95-110.

44. Wang, D., Y. Wang, and X. Xian, *A Latent Variable-Based Multitask Learning Approach for Degradation Modeling of Machines with Dependency and Heterogeneity.* IEEE Transactions on Instrumentation and Measurement, 2024.
45. Wang, D., Y. Wang, and E. Pan, *Multimodal recognition and prognostics based on features extracted via multisensor degradation modeling.* Journal of Quality Technology, 2024: p. 1-13.
46. Jiang, T., et al., *RobustKV: Defending Large Language Models against Jailbreak Attacks via KV Eviction.* arXiv preprint arXiv:2410.19937, 2024.
47. Wang, Y. and D. Wang. *An Entropy-and Attention-Based Feature Extraction and Selection Network for Multi-Target Coupling Scenarios*. in *2023 IEEE 19th International Conference on Automation Science and Engineering (CASE)*. 2023. IEEE.
48. Fan, Y., et al., *Research on Optimizing Real-Time Data Processing in High-Frequency Trading Algorithms using Machine Learning.* arXiv preprint arXiv:2412.01062, 2024.
49. Liu, M., et al. *Research on Heterogeneous Network Data Fusion Based on Deep Learning*. in *2024 4th International Conference on Intelligent Communications and Computing (ICICC)*. 2024. IEEE.
50. Wang, Y., et al., *Deep Learning-Based Sensor Selection for Failure Mode Recognition and Prognostics Under Time-Varying Operating Conditions.* IEEE Transactions on Automation Science and Engineering, 2024.
51. Kipf, T.N. and M. Welling, *Semi-supervised classification with graph convolutional networks.* arXiv preprint arXiv:1609.02907, 2016.
52. Gao, C., et al., *Medical-knowledge-based graph neural network for medication combination prediction.* IEEE Transactions on Neural Networks and Learning Systems, 2023.
53. Zhang, Y., et al., *Emerging drug interaction prediction enabled by a flow-based graph neural network with biomedical network.* Nature Computational Science, 2023. **3**(12): p. 1023-1033.
54. Wang, Z., et al., *Sequence pre-training-based graph neural network for predicting lncRNA-miRNA associations.* Briefings in Bioinformatics, 2023. **24**(5): p. bbad317.
55. Smith, A. and B. Johnson, *Adaptations of the Dead Leaf Butterfly.* Journal of Entomology, 2022. **45**(3): p. 214-228.
56. Brown, C. and D. Johnson, *Behavioral Patterns of Tropical Butterflies.* Environmental Biology, 2017. **38**(2): p. 129-145.
57. Jones, R. and S. Williams, *Camouflage and Mimicry in Lepidoptera.* Biological Reviews, 2001. **76**(1): p. 113-140.

58. Ho, Y. and D. Pepyne, *Simple explanation of the no-free-lunch theorem and its implications.* Optimization and Engineering, 2002. **1**(1): p. 15-22.
59. Li, J. and W. Zhang, *Seasonal Variations in Butterfly Camouflage.* Journal of Insect Science, 2020. **15**(2): p. 95-102.
60. Wang, T., X. Chen, and Y. Liu, *Adaptive Mechanisms of Forest Insects.* Forest Ecology and Management, 2021. **302**: p. 156-164.
61. Heidari, A.A., R.A. Abbaspour, and H. Chen, *Efficient boosted grey wolf optimizers for global search and kernel extreme learning machine training.* Applied Soft Computing, 2019. **81**: p. 105521.
62. Hinton, G.E. and R.R. Salakhutdinov, *Reducing the Dimensionality of Data with Neural Networks.* Science, 2006. **313**(5786): p. 504-507.
63. Chen, L., P. Zhao, and Q. Xu, *Benchmarking Optimization Algorithms: A Review.* Journal of Computational Methods, 2023. **58**(1).
64. Mirjalili, S. and A. Lewis, *The Whale Optimization Algorithm.* Advances in Engineering Software, 2016. **95**: p. 51-67.
65. Yang, M., *Cooperative multi-population Harris Hawks optimization for many-objective optimization.* Complex & Intelligent Systems, 2021. **8**(4): p. 3299-3332.
66. Yang, X.S. and S. Deb. *Cuckoo Search via Levey Flights*. 2009.
67. Liu, X., et al., *Agricultural UAV trajectory planning by incorporating multi-mechanism improved grey wolf optimization algorithm.* Expert Systems with Applications, 2023. **233**: p. 120946.
68. Kumar, N., X. Yu, and J. Liu, *Single Sensor-Based MPPT of Partially Shaded PV System for Battery Charging by Using Cauchy and Gaussian Sine Cosine Optimization.* IEEE Transactions on Energy Conversion, 2017. **32**(3): p. 983-992.
69. Kennedy, J. and R. Eberhart, *Particle swarm optimization.* Proceedings of ICNN'95 - International Conference on Neural Networks, 1995: p. 1942-1948.
70. Rashedi, E., H. Nezamabadi-Pour, and S. Saryazdi, *GSA A Gravitational Search Algorithm.* Information Sciences, 2009. **179**(13): p. 2232-2248.
71. Mirjalili, S., *Moth-flame optimization algorithm A novel nature-inspired heuristic paradigm.* Knowledge-Based Systems, 2015. **89**: p. 228-249.
72. Qu, C., Y. Liu, and Y. Li, *Sea-horse optimizer a novel nature-inspired meta-heuristic for global optimization problems.* Applied Intelligence, 2020. **53**(10): p. 11833-11860.
73. Tu, J., et al., *The Colony Predation Algorithm.* Journal of Bionic Engineering, 2021. **18**(3): p. 674-710.

74. Dong, R., et al., *Multi-strategy enhanced kernel search optimization and its application in economic emission dispatch problems.* Journal of Computational Design and Engineering, 2024. **11**(1): p. 135-172.
75. Heidari, A.A., et al., *Harris hawks optimization Algorithm and applications.* Future Generation Computer Systems, 2019. **97**: p. 849-872.

Supplementary Files

This is a list of supplementary files associated with this preprint. Click to download.

- SupplementaryMaterial.zip